Test Bench for Ultrasonic Sensing ASSP NCV75215

AND90239/D

Prepared by: Denis Zebrowski, Jiri Kantor, Dalibor Bartos

Summary

Nowadays ultrasonic time−of−flight measurement is successfully used in industrial and automotive applications. When reliability is a key aspect ultrasonic sensing has an advantage over camera detection. Its performance in low−visibility use−case is superior to infra−red cameras.

Due to small speed of an acoustic wave compared to low−range radar or light ray in lidar, questions arise whether it is worth to work on ultrasonic system that can mitigate doppler−effect as the acoustic wave is more susceptible to distortion than the other mentioned mediums. Apart from P215, the prerequisite for doppler radar is the ability to reliability determine and recalculate within milliseconds the relative distance based on the knowledge of doppler effect and the side−effects that it might be subject to. Dynamic control of the frequency at the receiver and transmitter of NCV75215 is already decoupled and the end−user should reliability identify the frequencies that correspond to a given relative speed and the distance between two objects.

onsemi, as a leading supplier of ultrasonic ASICs and the presented ASSP, is committed to delivering state−of−the−art sensing solutions for its customers.

Ultrasonic Measurement

The acoustic wave supported by the system is in the range of 35−90 kHz. In acoustics, the energy is described as sound pressure level (SPL). Acoustic wave propagation is a product of pressure created by vibrating a membrane in a gas. Frequency of vibration defines the frequency of the wave. The change in pressure (p) is inverse−proportional to distance (r) (inverse−distance law).

$$p \propto \frac{1}{r}$$

Time−of−Flight

NCV75215 ASSP (short: P215) is designed to process analog signal reciprocated from a nearby object and convert it into a digital information about its relative position. It can work with any ultrasonic transducer but the most used type is piezoelectric. P215 performs time−of−flight (TOF) measurement to detect the presence of and calculate the position of an object.

Detection range depends on several components:

- Piezoelectric ultrasonic transducer
- Matching circuit
- Digital tuning

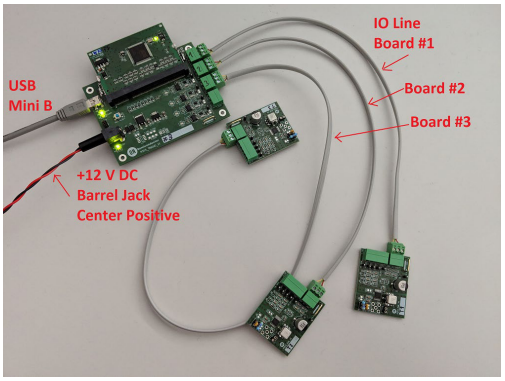

Figure 1. Testbench Photo

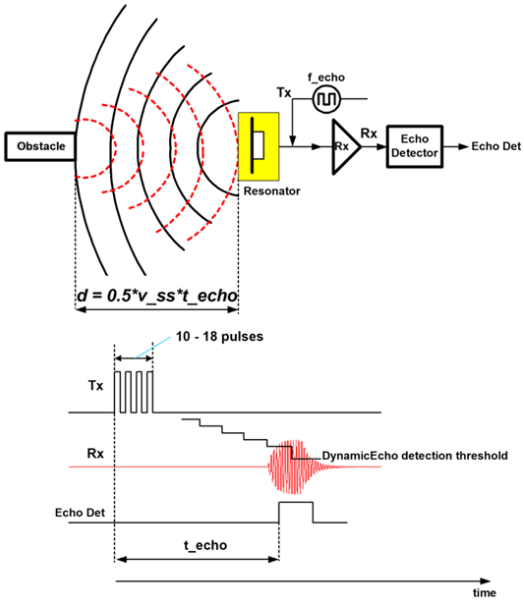

Figure 2. Ultrasonic Time−of−Flight Basic Representation

The NCV75215 can be tuned to a distance anywhere between 0.25 and 4 meters. As we will discover later, reverberations are the most crucial factor in the tuning process. They occur naturally after burst pulses and decay gradually over time. By monitoring them the ASSP can apply countermeasures which improve the range and reaction time. Under ideal external conditions and with a very−well tuned receiver, the ASSP can achieve detection at a distance as low as 20 cm.

Distance Estimation

Distance (d) is a product of measured time interval (t_{echo}) between burst pulse transmission and echo reception, and it is defined as half of the round−trip time of an ultrasonic pulse. Ambient temperature (T_{amb}) affects the density of atmospheric air and thus speed of acoustic wave (v_{sound}). The exact speed depends on the wave's period.

$$d = \frac{t_{echo} \cdot v_{sound}}{2}$$

Where:

$$v_{sound} \cong 346 \frac{m}{s} \text{ for } T_{amb} = 25°C \qquad \text{(eq. 1)}$$

E.g., for an object 1 meter away from the sensor, a burst pulse reaches the object after approximately 5.78 ms.

Reverberation

NCV75215 measures the reverberation period and the total length of the reverberation for diagnostic purposes. Based on this information the system can detect faults in the piezoelectric sensor.

Reverberation, depicted below, is a byproduct of burst pulse transmission. Thus, the control over the transmitted number of periods as well as the control over amplitude of the drive current is essential to accurately measure time of flight.

Multiple echoes are created and received at different timestamps by the transducer due to multipath effect.

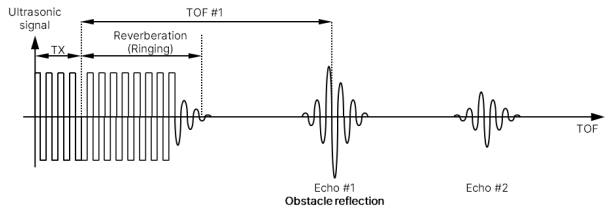

Figure 3. TX Burst Pulses, Reverberation, Echoes

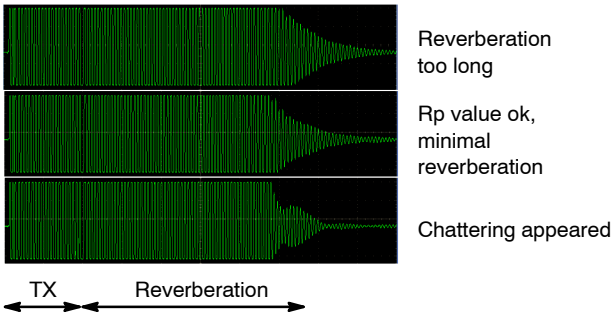

Figure 4. Reverberation Scenarios, 22 TX Pulses + Reverberation

Total reverberation time (t_{TX}) is a result of TX burst pulse count (n_{pulses}) and the carrier period (T_{pulse}), both of which are configurable in ASSP's software.

$$t_{TX} = T_{pulse} \cdot n_{pulses} \qquad \text{(eq. 2)}$$

Carrier period is defined by the oscillation frequency of the TX driver.

Equivalent Circuit

The piezoelectric circuit model can be represented as a structure of 2 resonators: serial and parallel. Both parallel and serial resonator should be tuned to the nominal resonant frequency of the piezoelectric transducer. Moreover, a tunable transformer can be selected to increase flexibility.

Serial Resonator

The resonant frequency of the circuit is defined by the serial resonator, i.e., transducer and can be calculated using its inductance (L_s), capacitance (C_s) and Thompson's formula.

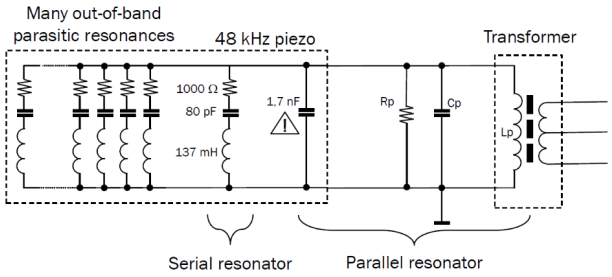

Figure 5. Equivalent Resonant Circuit of Transducer

Where:

f_R = 48 kHz, C_s = 80 pF, R_s = 1 kΩ, L_s = 138 mH, C_P = 1.7 nF.

Below Thompson's formula is applied to obtain resonant frequency. The values correspond with the picture.

$$f = \frac{1}{2\pi\sqrt{L_s C_s}} = \frac{1}{2\pi\sqrt{(80 \cdot 10^{-12}) \cdot 0.137}} = 48 \text{ kHz} \qquad \text{(eq. 3)}$$

Parallel Resonator

The same formula is applied to the parallel circuit model (L_p, C_p). Additionally, parallel resistance (R_p) significantly affects the reverberation time. Steps to tune parallel circuit:

1. Choose parallel resistance (R_p) to minimize reverberation time
2. Tune transformer and adjust parallel capacitance (C_p)

Trilateration and Object Detection

The goal in trilateration is to map an object on the cartesian plane defined by sensors. Two TOF measurements (d, i), below formulas (l_1, v_t) and knowledge of physical properties of an acoustic wave is sufficient for mapping.

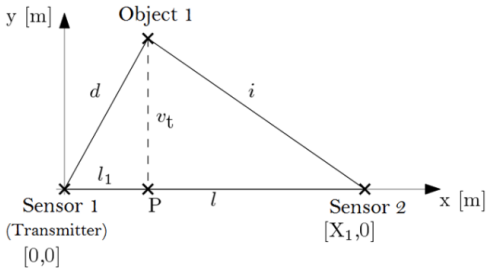

Figure 6. Trilateration Calculus

$$l_1 = \frac{d^2 - i^2 + l^2}{2 \cdot l} \text{ [m]}$$
$$v_t = \pm \sqrt{d^2 - l_1^2} \text{ [m]} \quad \text{(eq. 4)}$$

Once TOF is measured, the formula to find the distance to each sensor is simple. Applying trilateration is done by the central processing unit which collects the data from all the sensors.

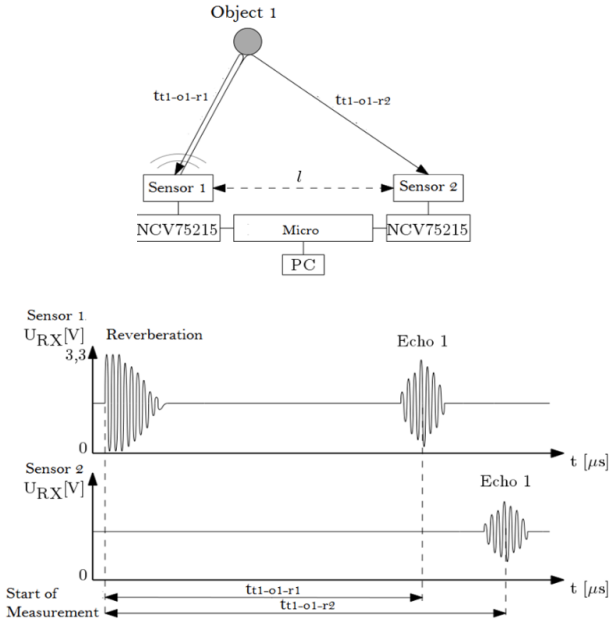

Figure 7. Extracting TOF Values using onsemi NCV75215

Indexes denote:

- $t_{t1-o1-r1}$ – TOF of a signal sent by sensor 1, reciprocated by object 1 and received by sensor 1, direct measurement. See variable d above
- $t_{t1-o1-r2}$ – TOF of a signal sent by sensor 1, reciprocated by object 1 and received by sensor 2, indirect measurement.

In the last step, calibration is necessary to assure the correct behavior of the overall system.

Direct vs. Indirect Measurement

Direct measurement is performed by the sensor which generates ultrasonic burst signal. Other sensors found next to it indirectly receive the reflections of the signal as it reciprocates under different angles in several directions (multipath propagation). Depending on object's position relative to sensors, the echo's magnitude at the receiver will vary among them.

During one measurement cycle, software analyses the received data from the sensors and determines the position of obstacles with the use of trilateration algorithm. It can use the data from two or three sensors. Starting from sensor S1, each next sensor transmits burst pulses.

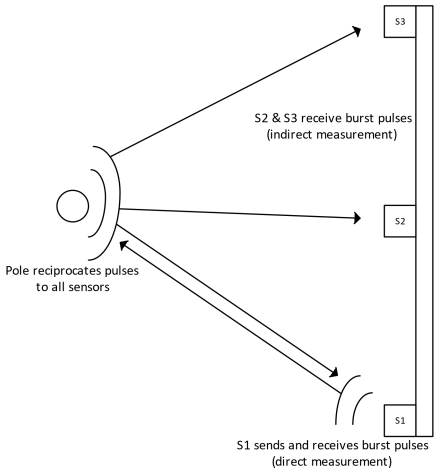

Figure 8. Direct and Indirect Measurement – 1 Cycle

It is necessary to utilize indirect measurements in trilateration. The measurement is arbitrated by the sensor responsible for sending ultrasonic burst signal. The end of transmission marks the start point of TOF measurement. The reception of direct and indirect echoes is logged by each sensor and reported to the master device. Distance between the sensors and the object is used for precise object localization.

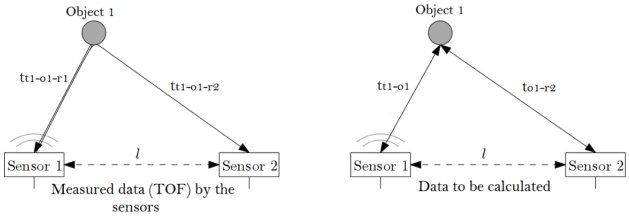

Figure 9. Measured vs. Calculated TOF Values

Time data is defined as per following equations:

$$\text{Direct (sensor1)} : t_{t1-o1} = \frac{t_{t1-o1-r1}}{2}$$
$$\text{Indirect (sensor2)} : t_{t1-o1-r2} - t_{t1-o1} \quad \text{(eq. 5)}$$

By using multiple sensors and indirect signals (multipath effect) more advanced use−cases, such as park assist, are feasible.

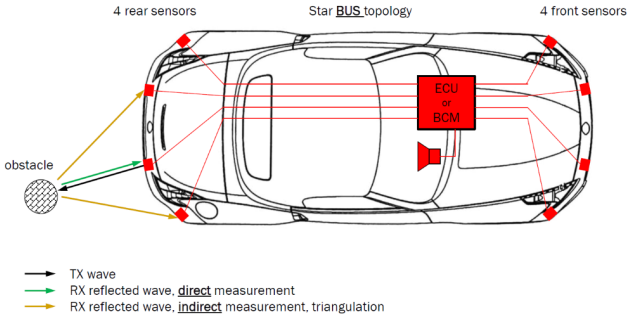

Figure 10. Car Park Assist Use−case

Confirmation Algorithm

Selection of algorithm type depends on the end application and complexity of the measurement. In general, double confirmation scheme offers more robustness as it requires less sensor signals. However, if the intention is to achieve maximum accuracy, the measurement area is narrow and placed centrally, a triple confirmation scheme is recommended.

Double confirmation scheme:

- Input from 2 sensors sufficient
  - ♦ wider detection angle,
  - ♦ better minimum distance,
- Faster confirmation but more false positives.

Triple confirmation scheme:

- Input from 3 sensors
  - ♦ narrower detection angle,
  - ♦ worse minimum distance,
- Slower confirmation but more stable, i.e., fewer false positives.

The multi−sensor approach enlarges the detection area compared to one sensor always acting as a transmitter. It also discards false echoes more efficiently as it requires object confirmation from at least 2 sensors in 2 consecutive measurements (double confirmation algorithm). In the case of simple use−cases, such as occupancy detection, where narrow viewing angle is sufficient, single−sensor approach can be used.

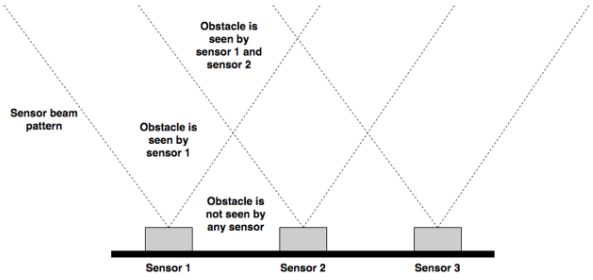

Figure 11. Sensor Viewing Area

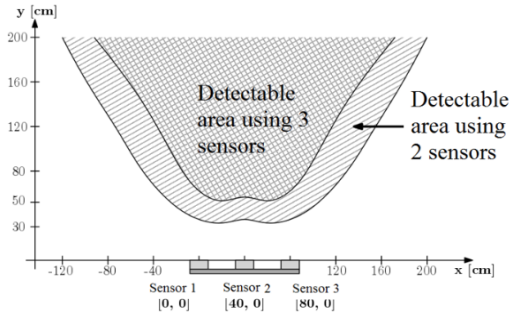

Figure 12. Overlap between Viewing Areas

The Figure 13 shows a sequence consisting of 9 steps during which the overlap point between signals from 2 sensors and in effect length v_t is found.

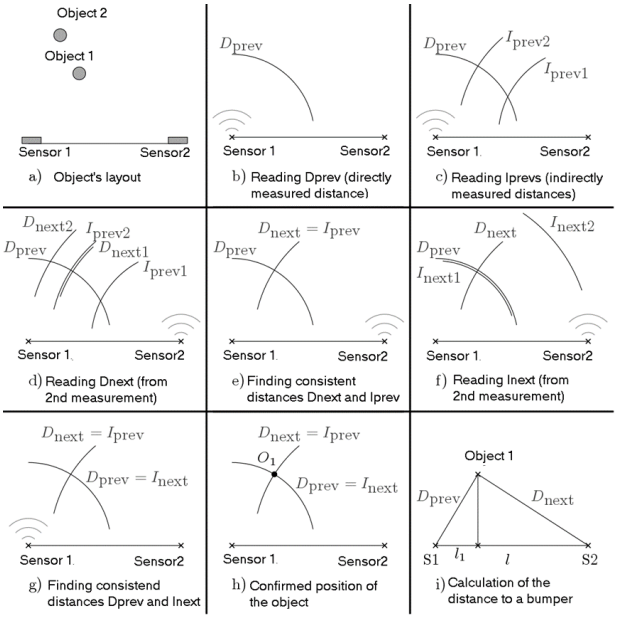

Figure 13. Measurement and Localization using Trilateration − Sequence

In the study, only the double conf. algorithm is evaluated in detail. In principle, an object is successfully localized if the coordinates calculated from both pairs of sensors (sensor 1 + 2 and sensor 2 + 3) overlap within the tolerance region. This setting is particularly good for obstacles in short distances, it can find the position if the obstacle is just 25 cm away from the sensor.

The triple confirmation shows better results for longer ranges, i.e., exceeding 3 meters. Data from all three sensors is used to find the position of the obstacle. It is more stable and less susceptible to false echo position detection. Because all three sensors need to see the obstacle, the minimum distance at which it can localize the obstacle is further away (approx. 35 cm) but it strongly depends on the transducer.

Software implementation of both methods is defined in trilateration.cpp.

Moving objects with uneven surfaces might yield different results in 2 consecutive measurements. For the algorithm to accommodate such use−cases it is necessary to identify tolerances and define spatial boundaries within which the object is labelled as found.

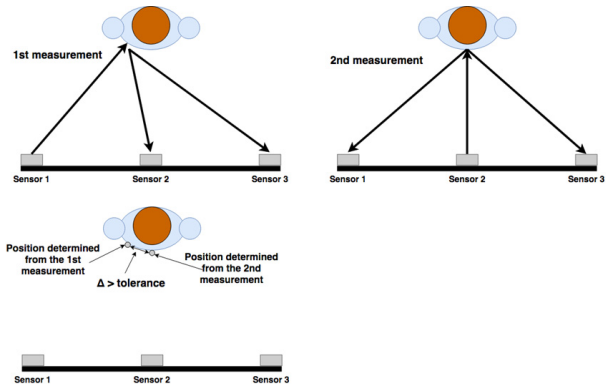

Figure 14. Human Detection Requires Fine−tuned Algorithm

To summarize:

1. For detection of the object in two−dimensional space at least 2 sensors are mandatory.
2. To confirm location of the obstacle at least 2 consecutive measurements by each sensor are necessary.
3. It is essential to confirm the sensor's viewing angle and resulting detection range on testbench if other than recommended sensor is to be selected.

P215 Evaluation Kit

The schematic is based on the recommendations from the datasheet. Auxiliary elements include center−tapped transformer connected via its primary side to TX driver's output pins (DRVA/B/C). The secondary side feeds the piezoelectric element and connects via the matching circuit (C4, R5) and capacitive coupling (C1/5) to RX input pins. No EMC filtering is available.

Receiver Path Routing

The external components of the receiver are located on the left side of the ASSP and are recommended to be placed close to RX pins. Also, the analog ground plane (GNDA), that these components are connected to, should be separated from the digital ground on the right side of NCV75215 EVK. To prevent the electromagnetic field (EMF) of the RX path from coupling the surrounding noise, the RX path should be routed inside of the poured GNDA polygon that acts as EM shielding. These routing practices help to achieve a better signal−noise ratio (SNR) at the receiver.

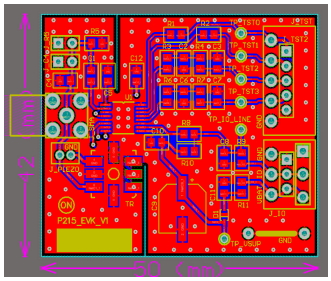

Figure 15. Top Layer

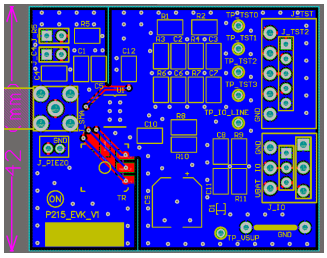

Figure 16. Bottom Layer

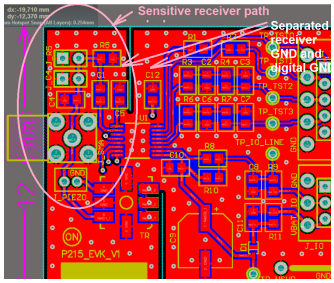

Figure 17. RX Part of PCB

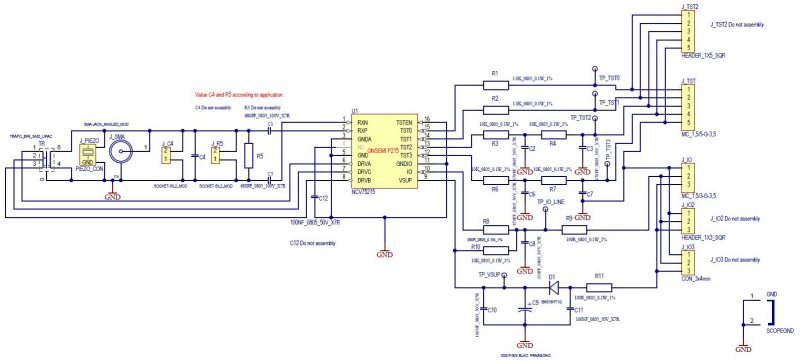

Figure 18. Sensor Board with NCV75215

Test Pins

Test pins TST 0−3 serve for application debugging. TST2 and TST3 are PDM debugging ports that allow to observe echo magnitude, detection etc. A full list is provided in the NM Register Control tab of P215 Qt graphical interface.

PDM debugging ports are filtered by a 2nd order LPF. In end−design these pins should be connected to digital ground as they can pick up noise, due to high−speed signal slopes.

Assembled Demo Boards

The demo sensor board is based on NCV75215 module from onsemi and was tested with Murata 58 kHz MA58MF14−7N transducer. Recommended list of transducers can be found in the datasheet of NCV75215.

To achieve optimal reverberation time, we calculate the values of the parallel resistor and capacitor in the matching circuit.

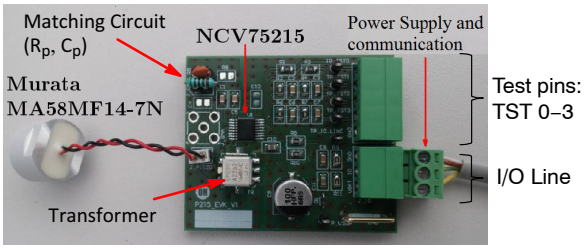

Figure 19. Sensor Demo Board

The master board connects to the sensor boards via four (4) NCV7321 LIN transceivers from **onsemi**. An Atmel AVR32 microcontroller controls the measurement, extracts the detected echoes from sensors (NCV75215 slave modules) and sends them to the PC software for analysis.

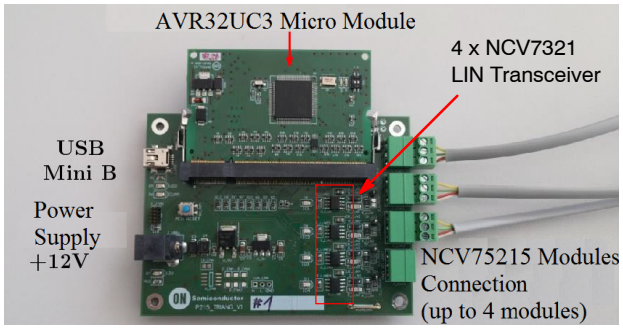

Figure 20. Master Demo Board

Up to four (4) NCV75215 modules can be connected to the main master board. The master board requires approx. 12 V and 100 mA. Depending on the number of connected sensors the current consumption will vary.

Table 1. POWER CONSUMPTION

Number of Sensors	Power Consumption [mA]
0, no USB	71
0, USB	79
1	83
2	90
3	94

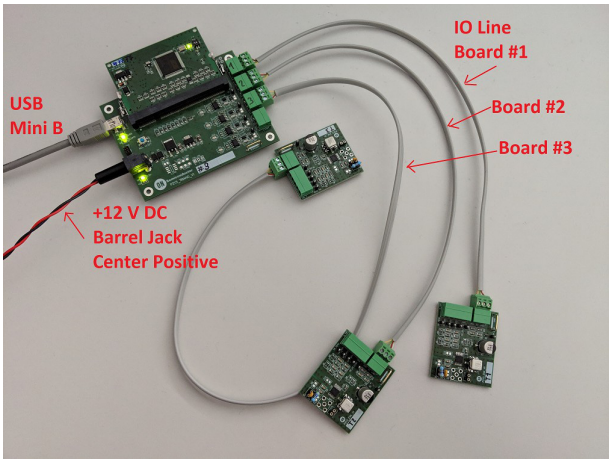

Figure 21. Complete Setup with 3 Out of 4 Sensor Boards

The boards work correctly if the serial port of the connected master board is displayed in Trilateration demo software.

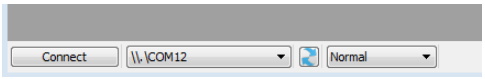

Figure 22. Connection Successful

NCV75215 ASSP

The ASSP device controls the ultrasonic transducer (P_{Z1}) via a transformer (T_{r1}). The receiver's path impedance is defined by the matching circuit (C3). Additionally, EMC filtering (C_{F1}, R_{F1}, R_{F2}) is added before the input pins. Moreover, 2 capacitors (C1, C2) serve as capacitive coupling of the receiver.

The blocks in the diagram represent the functionalities constituting either the analog front−end or digital signal processing (DSP) unit. The analog signal from ultrasonic transducer is amplified (LNA & VGA), converted to digital (ADC). At the digital side, the signal is filtered (BPF) before comparing it to a time−dependent threshold (Threshold control) which defines the detection threshold of an echo.

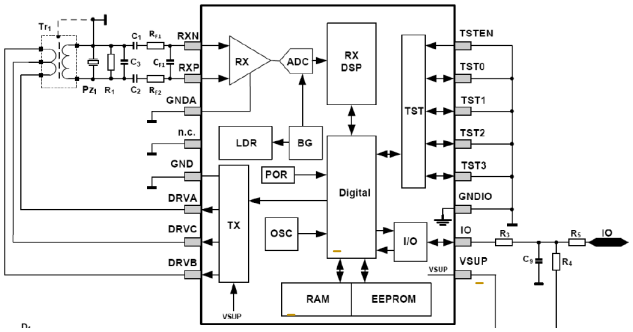

Figure 23. ASSP Diagram

The echo is reported on I/O Line (IO Line transceiver) when the signal magnitude exceeds the threshold.

Steps and corresponding output signals:

1. Receive analog RX signal → RX analog
2. Convert analog RX signal to digital
3. Amplify it with dynamic gain (VGA)
4. Apply filtering → Echo Magnitude
5. Apply threshold detection → Echo Envelope
6. Debounce → Echo Detection

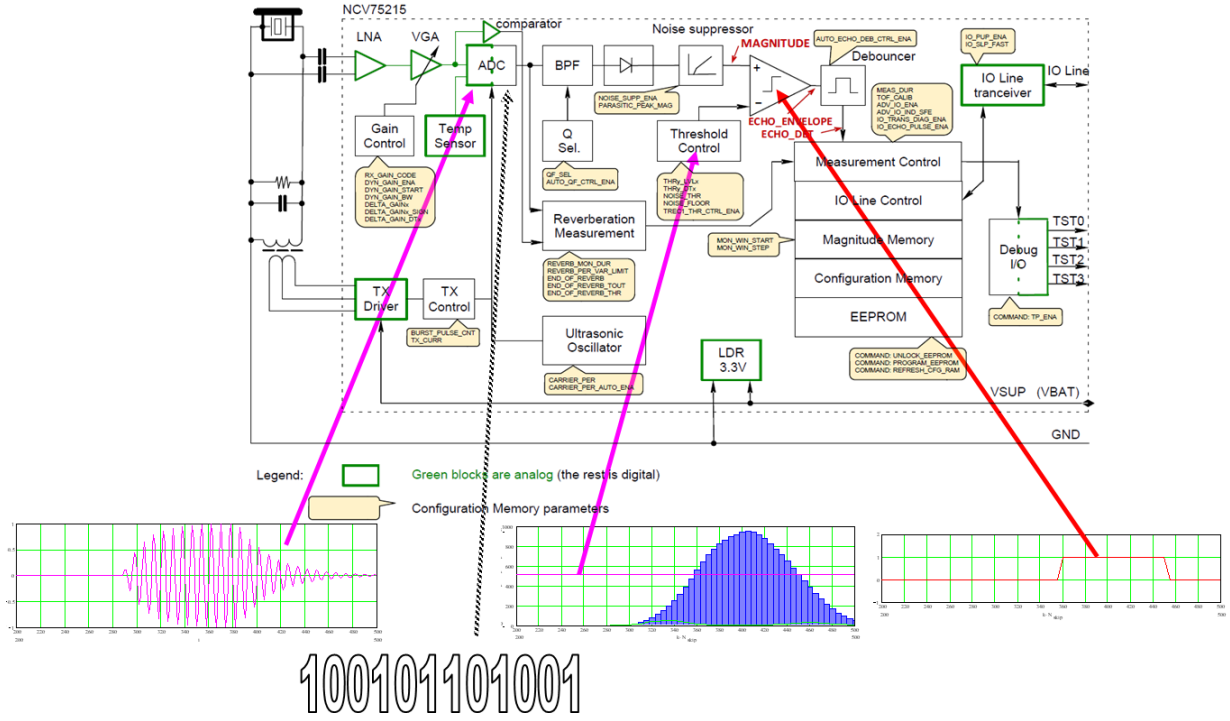

Figure 24. Signal Processing Block Diagram (Ref. Datasheet)

Supply Voltage, Drive Current, Burst Power Saturation

The Figure 25 shows an example of drive current and supply voltage characteristic of the NCV75215. The minimum voltage level (V_{supmin}) defines the transmit power for the transducer. If the transducer's equivalent serial resistance (R_{Smax}) is too high, it limits both V_{supmin} and thus drive current (I_{TX}) as per the characteristic.

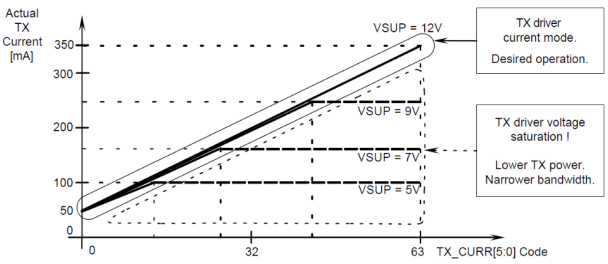

Figure 25. Example of Vsup (I_{TX}) Characteristic

The relation between the transmit current and voltage changes, depending on the transformer and the impedance of its primary winding.

Figure 26. Center−tapped Transformer

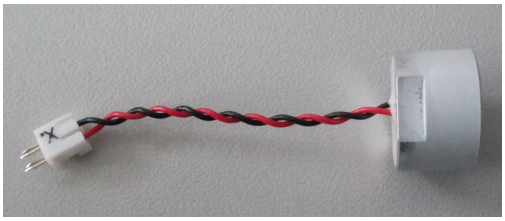

Figure 27. Transducer Murata MA58MF14−7N 58 kHz

We should adjust transformer turn ratio and resonant circuit characteristics to avoid the saturation of V_{sup} voltage which eventually leads to lower transmit power. Minimum supply voltage (V_{supmin}) is described as follows:

$$\begin{cases} V_{sup_{min}} = V_{'DRVC_{On}} + V_{DRVA,B} + V_{S_{max}} \\ V_{S_{max}} = \dfrac{R_{S_{max}} \cdot I_{TX}}{N^2} \\ V_{DRVC_{On}} = R_{DRVC_{On}} \cdot I_{TX} \end{cases}$$

$$V_{sup_{min}} = V_{DRVC_{On}} \cdot T_{TX} + V_{DRVA,B} + \frac{R_{S_{max}} \cdot I_{TX}}{N^2} \quad \text{(eq. 6)}$$

Where:

R_{DRVCOn} − switch on resistance at TX driver output C (center of the winding),
I_{TX} − TX current,
$V_{DRVA,B}$ − voltage between TX driver output A and B (primary winding),
R_{smax} − transducer maximum equivalent serial resistance,
N − transformer turn ratio e.g., 1:1:8 → 8 (step−up 8 times),
V_{supmin} − TX voltage (secondary winding).

An example of how to calculate the minimum supply voltage to avoid TX saturation.

Known values: I_{TX} = 350 mA (maximum), R_{Smax} = 1000 Ω, N = 8 (1:1:8), $V_{DRVA,B}$ = 2 V, R_{DRVCon} = 3.7 Ω (maximum).

$$V_{sup_{min}} = 3.7 \cdot 0.35 + 2 + \frac{1000 \cdot 0.35}{8^2} = 8.76\ V$$

The transformer acts as a push−pull converter for the transmitted burst pulses and received echoes. The center tap (CT) of the transformer divides the primary coil in half. The voltage measured between one end and the center tap of the primary side is N times higher on the secondary side. This can be calculated as follows:

$$V_{sec} = \frac{N_{sec}}{N_{pri,CT}} \cdot V_{in}$$

Example:

N_{sec} = 8, $N_{pri,CT}$ = 1 (1:1:8), $V_{DRVA,\,B}$ = 2 V → V_{sec} = 8 V.

Transformer Requirements

The NCV75215 controls a piezoelectric membrane that vibrates under applied drive current (ITX). Tuning to the desired frequency is only possible if the components were chosen correctly. We present the typical values of the transducer and transformer for a given resonant frequency.

Typical values:

- Secondary inductance: 3 to 5 mH,
- R_{dc} Secondary: 25 to 50 Ω,
- R_{dc} Primary: 1.6 to 2.5 Ω,
- No. of turns ratio (pri_A:pri_B:sec): 1:1:8 to 1:1:11.

Transducer & Matching Circuit Requirements

Typical values:

- Resonant frequency: f_R = 48 to 58 kHz,
- Parallel capacitance: C_p = 22 pF to 4 nF,
- Parallel resistance: R_p = 3 to 8.2 kΩ,
- Series resistance: R_s = 1 to 2 kΩ.

The evaluation kit works both with tunable and non−tunable transformer. Parallel resistor (R_P) and capacitor (C_P) correspond to R5 and C4 respectively (schematic).

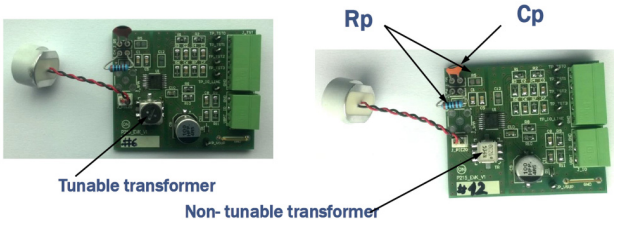

Figure 28. Transformer and the Matching Circuit

Detection Threshold

Threshold is part of digital signal conditioning, and it defines a minimal magnitude level of a received signal at which the received echo signal is detected as an object. Anything below the threshold value is ignored.

Threshold curve is linearly interpolated and consists of 12 sections – for each section, a level and its duration are specified.

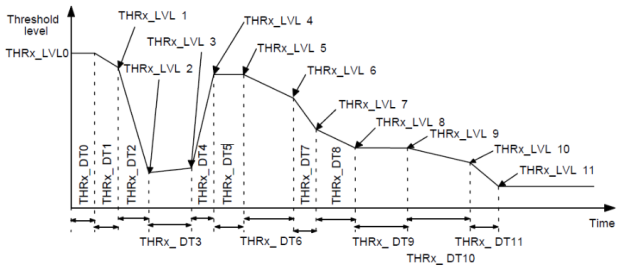

Figure 29. Threshold Curve (ref. Threshold)

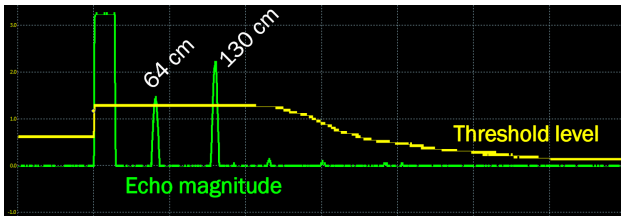

Figure 30. Example of Threshold and RX Signal on Oscilloscope

Dynamic RX Gain

Dynamic gain is part of analog signal conditioning and is essential to keep the received analog signal within the dynamic range prior to digital processing steps. Gain is controlled dynamically so that weaker echoes that arrive from more distant objects are interpreted correctly. This method enlarges the detection area of a sensor.

Dynamic gain shown in Figure 31 consists of 5 sections. Each of them is defined by starting gain, gain delta and time duration.

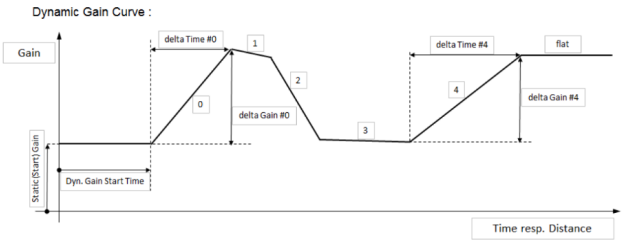

Figure 31. Dynamic Gain Curve (ref. Datasheet)

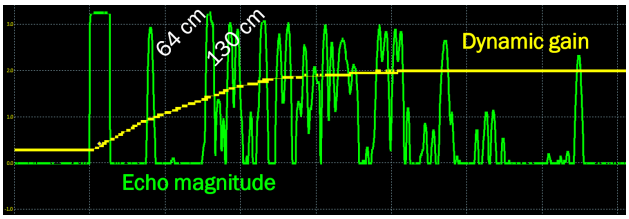

Figure 32. Example of Dynamic Gain and RX Signal on Oscilloscope

IO Line Data Communication

An IO driver controls the IO line to provide communication between an ECU and the NCV75215.

IO Line Properties:

- 3.3 kbit/s baud rate,
- 8−bit checksum,
- Pulse Width Modulation (PWM) bit coding,
- 4−bit addressing.

There are 3 types of communication that are possible with NCV75215:

- Standard: reports reverberation and echo with their actual width by pulling the bus voltage down to ground,
- Echo reporting: reports the same information with short pulses thus optimizing the bus usage,
- Advanced: no echo reporting on the bus while the measurement is ongoing. Instead, data communication is used afterwards to encode the information about the peak duration. This method also reduces disturbances on the bus and in DSP.

Low state on the bus is used to encode information (zero−dominant) when the bus transmits in advanced mode. IO−Line encoding takes place in a predefined fixed−time frame and is analogical to LIN communication. This mode is enabled via register 10− “Advanced IO Line protocol enable” bit.

Rising and falling edges have slope control function to reduce EMI radiation. This slew−rate control is disabled (IO_SLP high) after 60 µs (typical, T_{SLP_IOL}).

During the measurement cycle, the driver asserts a low level (IO_CMP) on IO Line (IO) which indicates that an echo is detected. After the end of measurement cycle the internal logic turns the control block off.

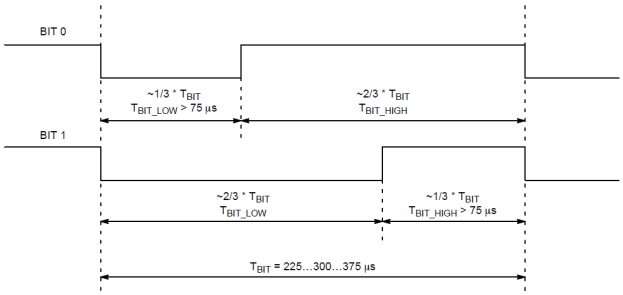

Figure 33. Single Data Frame used by Advanced IO−Line Mode

The integrated low−side driver requires an external pull−up resistor (R4) connected to V_{SUP}.

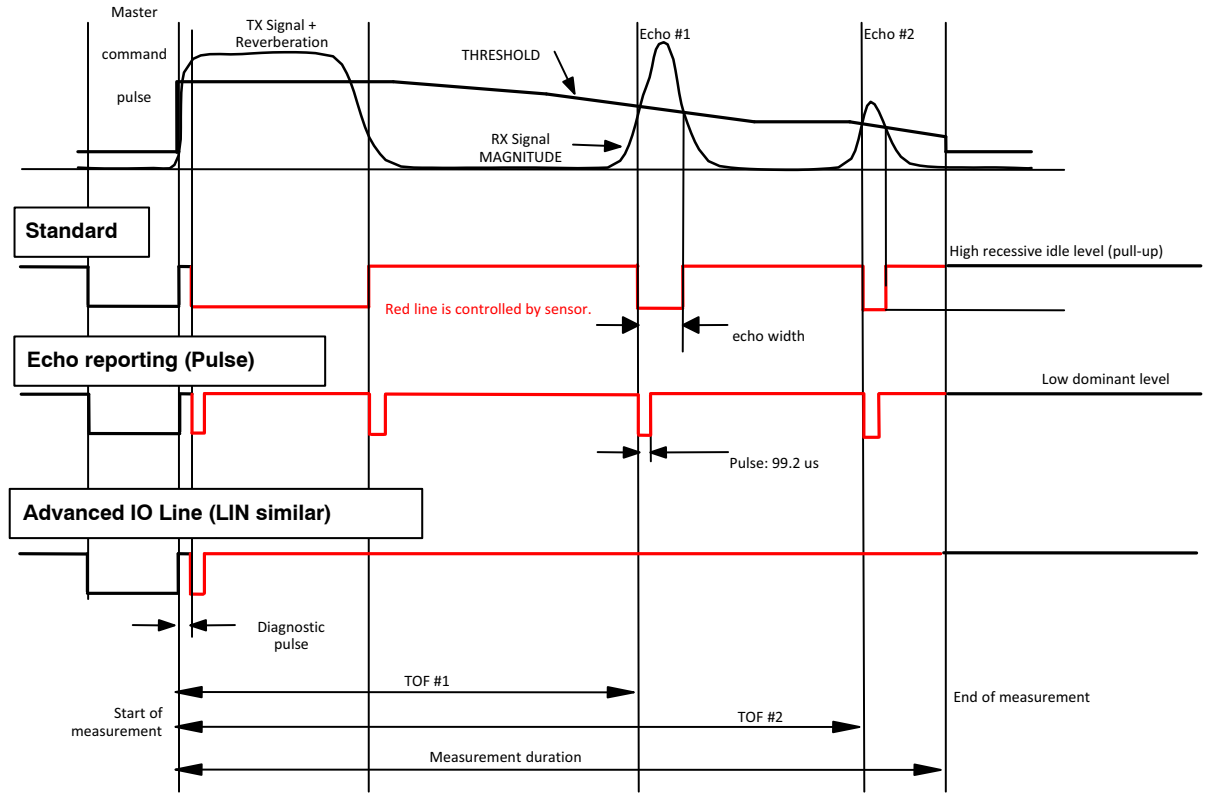

Figure 34. IO− Line Communication − Standard, Advanced, Echo Reporting

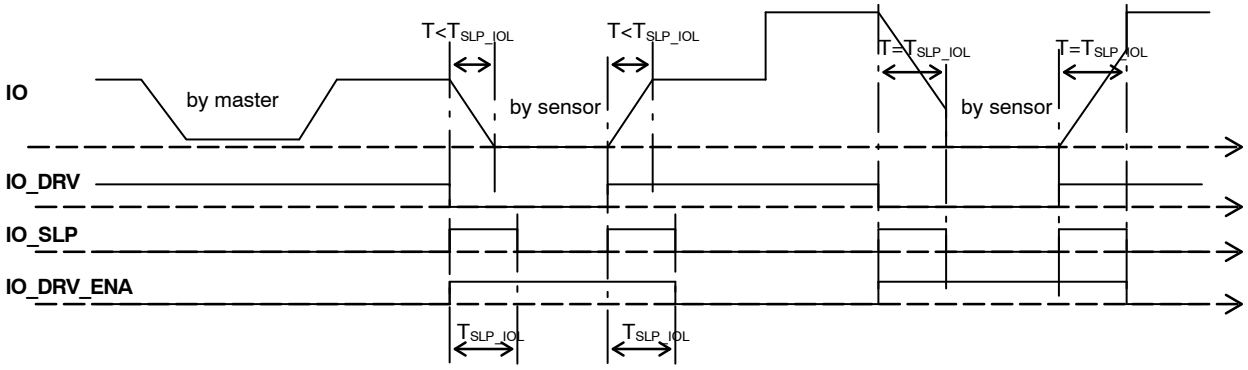

Figure 35. Timing of IO−Driver Inputs/Outputs. Example: Sensor controls the IO Line

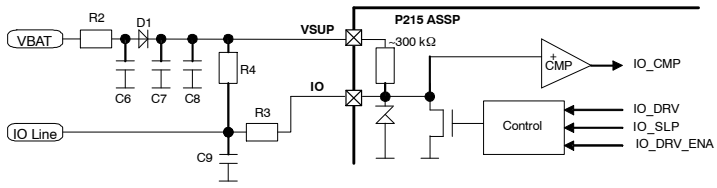

Figure 36. IO−Line Internal Driver with External Network

Table 2. PARAMETERS OF IO/LINE COMMUNICATION PROTOCOL

Parameter	Min	Typ.	Max	Unit
Output Slew Rate		0.5	0.8	V/μs
I/O Short Circuit Current	10		50	mA
Pull−up Resistor	200			kΩ
Duration of slew rate control		60		μs
IO line recessive current consumption			150	μA
IO line dominant current consumption			600	μA

Master MCU Firmware

The MCU controls the measurement, extracts the detected echoes from sensors and sends them to the PC software for analysis.

Front−end Qt Application

This tool communicates with AVR32 microcontroller over the serial line (UART).

Configurations include:

- Resonant frequency,
- Measurement mode,
- Threshold and dynamic gain,
- IO−Line settings.

Qt Application consists of 3 Windows:

1. “Measurement” menu – basic control of the measurement such as start/stop.
2. “Triangulation” menu – presents the results in graphical form in cartesian coordinate system.
3. “NM Controller (NM)” menu – configures EEPROM registers.

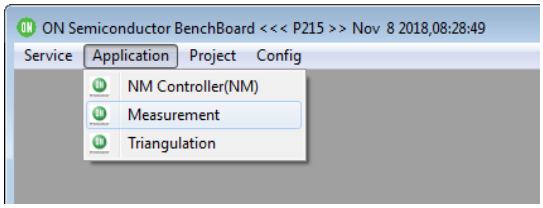

Figure 37. Three Application Windows

Although the software references “triangulation”, the underlying method is based solely on trilateration principles. No angle is measured or calculated in the process.

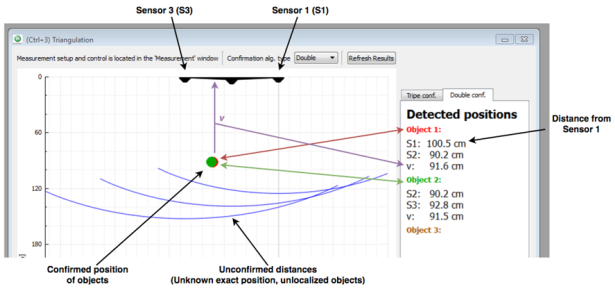

Figure 38. Trilateration Real−time Measurement Window

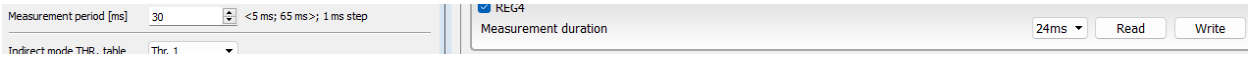

Figure 39. Measurement Period and Duration Values in Qt Software, NM Controller

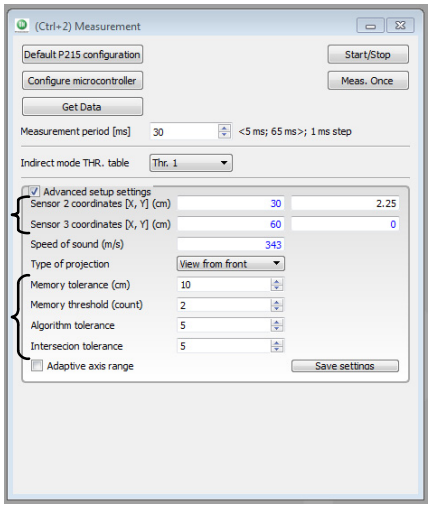

Start/Stop Continuous Measurement

Perform Single Measurement

Sensor location [x, y] relative to sensor 1

Algorithm/trilateration settings

Figure 40. Measurement Configuration Window

Figure 39 shows:

- “Measurement period” setting influences the speed at which the measurement is repeated. It must be longer than the “Measurement duration” in “NM Controller” window.
- “Memory threshold” & “Memory tolerance”– not implemented.
- “Algorithm tolerance” – specifies tolerance for declaring confirmation during comparison of 2 consecutive measurements from the same sensor.
- “Intersection tolerance”– used by triple confirmation. Object is detected upon intersection ± tolerance of arches/circles. The radius of a circle is equal to the distance from an object to each sensor.
- The coordinates refer to the position of the sensors relative to sensor 1, i.e., [0, 0].
- “Adaptive axis range” setting is used for measurements at longer distances.

“NM Controller” menu from Figure 42 offers optional advanced configuration of NCV75215 through its 16 registers in EEPROM. For basic demonstration purposes with an object in specified range it is not necessary to modify their content, nevertheless several settings that help to optimize the measurement are demonstrated.

The value of duration is stored in register 4 (REG4). The period must be greater than meas. duration.

The selection of test pin output signal is stored in register 15 (REG5).

- Echo detection,
- Echo magnitude,
- Echo threshold,
- Echo gain.

Pin 0 can be changed between amplified differential signal from transducer (“RX Analog”) or high−impedance signal from the transducer passed through a pull−up resistor (“HiZ”). Pin 1 can be skipped.

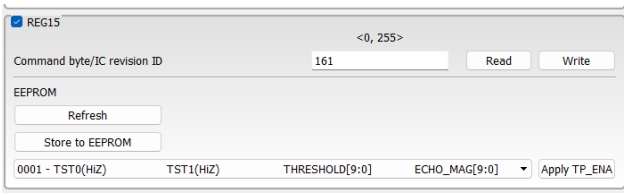

Figure 41. Test Pin Signal Assignment, NM Control

In register 10 (REG10) sensor current or reverberation debounce time are among the settings that can improve reaction time and detection range. Users might decrease sensor current to avoid saturating TX power which could lead to longer reverberation time and chattering effect. Debounce time is another measure to tackle this issue and improve robustness. Remaining parameters in REG10 deal with reverberation monitoring and digital post−processing of the received echoes.

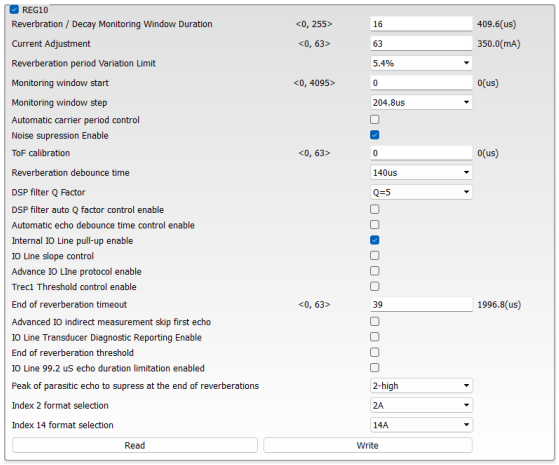

Figure 42. Reverberation Control and Additional Settings, NM Control

Table 3. ADDITIONAL PARAMETERS TO IMPROVE PERFORMANCE, REGISTER 10 SETTINGS

NM Window Label	Description	Software Variable (REG10)	Default State
• Reverberation / Decay Monitoring Window Duration • Monitoring window start • Monitoring window step	Reverberation monitor: start time, duration, and accuracy. Should be set accordingly to sensor's behavior.	REVERB_MON_DUR[8], MON_WIN_START[12], MON_WIN_STEP[2]	[duration, start, step] = [409.6, 0.0, 204.8]
Reverberation period Variation Limit	In case variation is above specified limit error flag is set. Serves as automatic sensor check.	REVERB_PER_VAR_LIMIT	5.4%
Noise suppression Enable	Measure to improve Signal−Noise−Ratio	NOISE_SUPP_ENA	1
Automatic carrier period control	Ensures the optimal sensitivity and SPL of the transducer over temperature, instead of manual tracking of reverberation frequency. Might require higher IO−Line bandwidth to during active measurement.	CARRIER_PER_AUTO_ENA	0
DSP Filter auto Q factor control enable*	Automatic control of Q factor. Measure to improve detection performance during dynamic ranging and at longer distances.	AUTO_QF_CTRL_ENA	0, fixed Q = 5
Automatic echo debounce time control enable	Improves detection during dynamic ranging (similarly to auto Q factor control). Use only with auto Q factor control and adaptive axis range enabled.	AUTO_ECHO_DEB_CTRL_ENA	0

*Higher Q results in less losses at the resonator due to more damping of parasitic frequencies (acts as a filter) and effectively in better SNR. It is recommended for greater detection distance thus echo detection in dynamic environment can be improved.

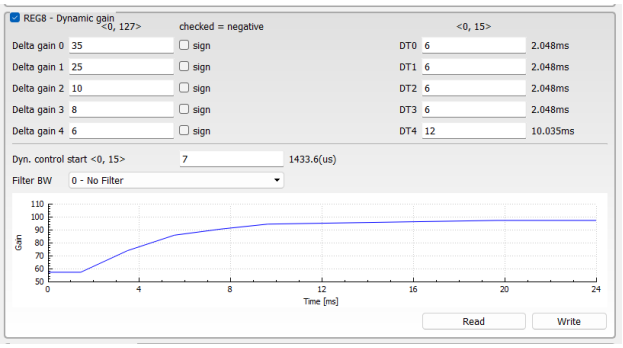

Figure 43. Dynamic Gain Values, NM Controller

Register 5 and 8 store gain and threshold values. The curves are modelled underneath using linear interpolation.

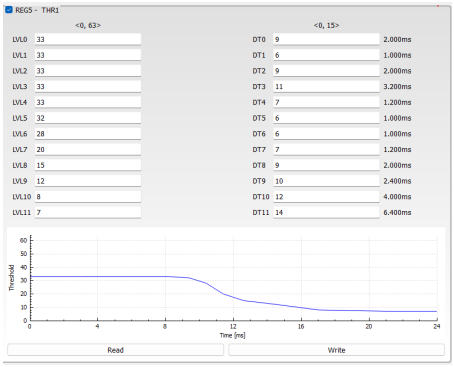

Figure 44. Threshold Register Values, NM Controller

Tracking of transducer temperature is especially useful for keeping the performance of the transducer flat over temperature. Due to change in temperature, SPL varies, and the receiver's sensitivity should be readjusted. This can be done using temperature reading from the pins connected to the transducer and stored in register 0. This value can be used to return the RX gain and for automatic carrier period control (see above).

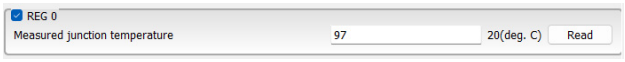

Figure 45. Transducer Temp. Reading is Possible over Connected Pins

TX & RX period can be controlled independently from each other which makes it possible to turn the P215−based system into doppler radar.

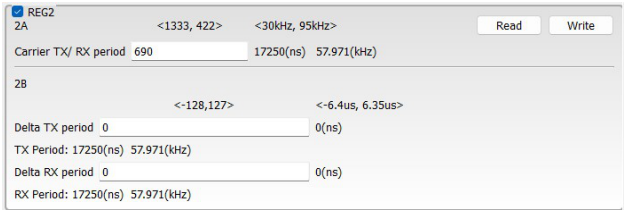

Figure 46. TX & RX Period can be Controlled Independently

Back−end C++ Application

"Measurement.cpp" contains the functions that are called within "Measurement" menu in Qt application. Except for basic start/stop measurement command, it provides interface to set more advanced meas. parameters such as meas. period. The data received from Qt app. is passed to the other two C++ applications which are explained in the next sections.

Finding Obstacles

"Trilateration−cpp" defines functions that analyze the measurement data samples and calculate the position of obstacles with use of selected algorithm. Both algorithms are supported by the code.

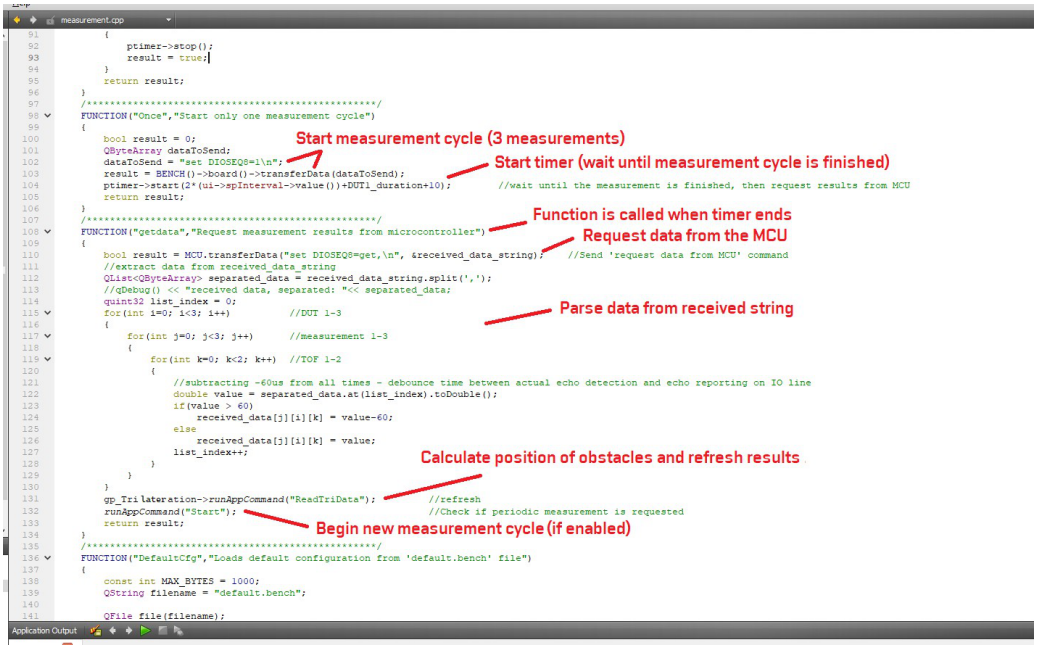

Figure 47. Data Processing between MCU and Qt GUI in measurement.cpp

NCV75215 Configuration & Control

NM Controller is a graphical interface that wraps up the functionalities defined in "tmccontroler.cpp" C++ application. Registers R0−R15 of NCV75215's EEPROM are read and written by AVR32 MCU over IO−Line. AVR32 executes the user commands coming from the Qt application and reports back the register status when possible. Beside read/write register operations, C++ source file contains also functions to control status LEDs of the master board via DIO pins.

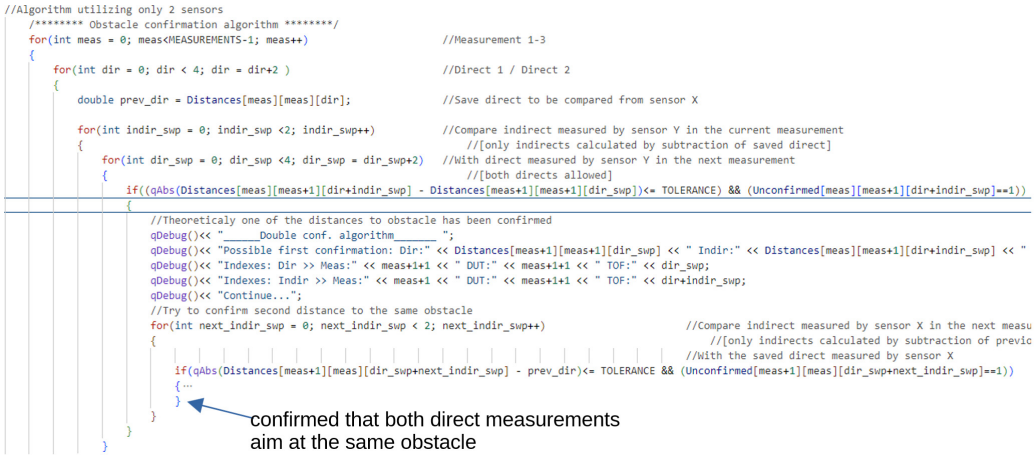

Figure 48. Snippet of Double Confirmation Algorithm Loop in "trilateration.cpp"

Measurement Test Bench

"P215_EVK_V1" sensor boards are connected in star topology to "P215_TRIANG_V1" master board. Three sensors are sufficient for demonstrating trilateration, whereas 4 sensors increase the detection area.

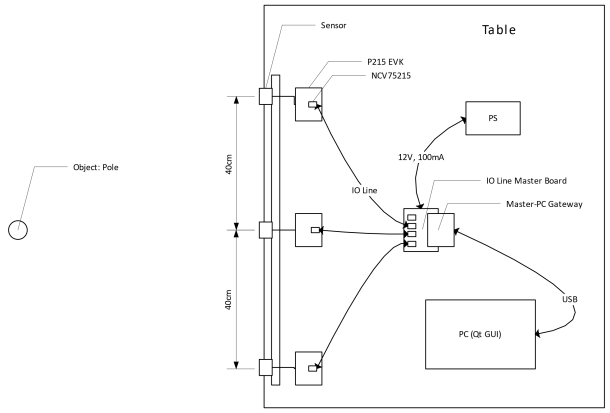

Figure 49. Top View Drawing

Figure 50. Front View

Figure 51. Side View

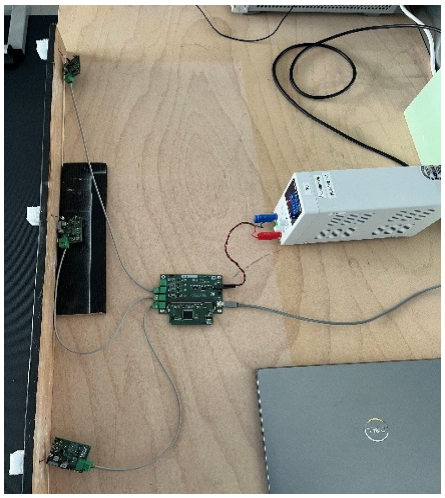

Figure 52. Top View

Trilateration Range

The maximum detection range was limited due to the laboratory's constrained environment. Nevertheless, it can provide insight into system's capabilities in complex use−cases with multiple objects that can reflect the acoustic wave.

For test purposes we focus on demonstrating out−of−the−box detection performance of the ASSP. Therefore, only default configuration was used to generate results. Results showed that depending on the object's position, the detection range varies. It reaches its maximum point of 2.8 meters midway of the testing area.

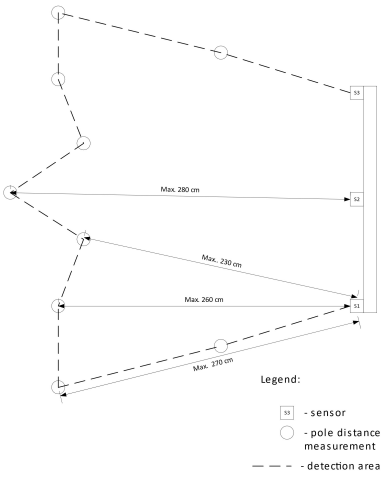

Figure 53. Object Detection Range Measured in the Lab

Measurement Period & Duration

Measurement period and cycle are shown below with 3 IO−Line V_{bat} signal curves (yellow, green, purple) − each assigned to a different sensor. To represent meas. duration, we use an additional diagnostic signal (pink) indicating when the measurement is ongoing. The measurement cycle consists of 3 meas. periods. Each period is configured by default to last 24 milliseconds. Three sensors transmit in alternating round−robin fashion.

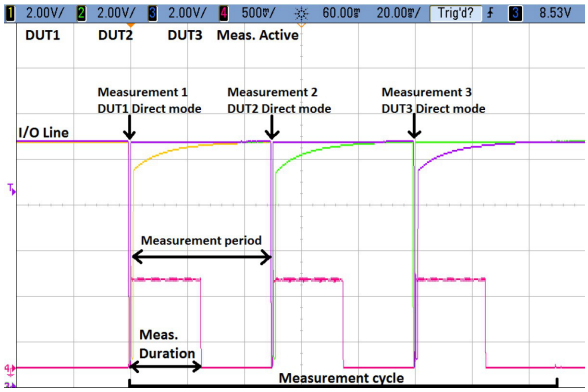

Figure 54. Measurement Duration, Period, and Cycle

When the first sensor is in direct measurement mode, its battery voltage drops during the transmission of burst pulses by approx. 1.1 V and recovers to its nominal value (blue curve) of approx. 12 V. IO−Line communication is dependent on the battery/power supply voltage level. We observe several square−shaped voltage drops (red curve). The first low voltage state represents TX transmission followed by a few dips indicating detected echoes, each of different length. Yellow and green curves represent the same behavior for the second sensor. The measurement period for both signals in the case is 30 ms.

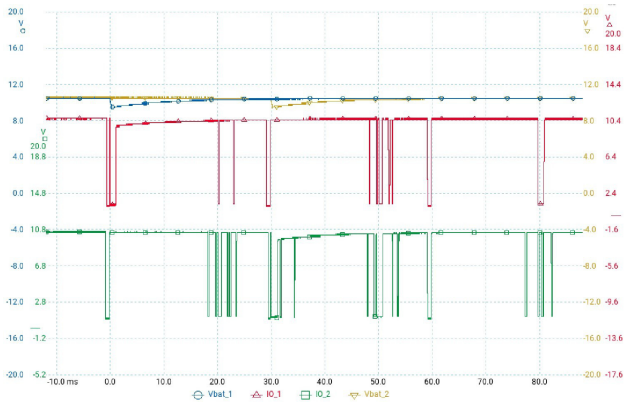

Figure 55. Echo Detection Encoding on IO−Line

Threshold Visualized

The threshold curve (red) is a digital reference signal compared with echo's magnitude. Its purpose is to filter out irrelevant echoes. In the case of objects located further away there is a visible difference in arrival time and magnitude of an echo. The green curve starts with TX burst pulse from sensor 1 followed by multiple echoes. Three identical red shapes correspond to 3 measurement periods, i.e., TX+RX slots − each reserved for different sensor.

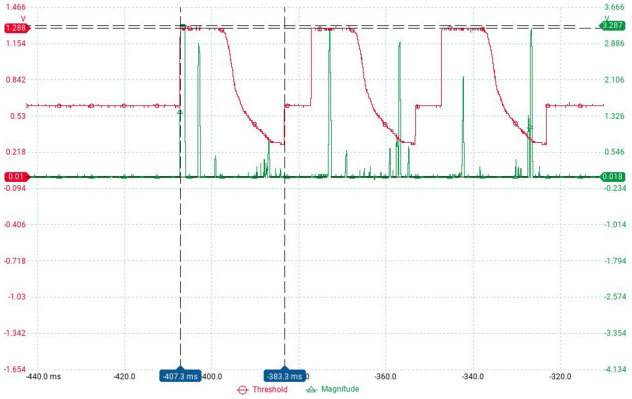

Figure 56. Pole 70 cm Away, Threshold and Magnitude, Measurement Duration of 24 ms

Figure 57. Pole 2.3 m Away, Threshold and Magnitude

Dynamic Gain

The gain curve defines the sensitivity of the receiver path, i.e., the amplification of the analog RX signal. Like the detection threshold, the gain curve is also fully configurable. Gain value is set based on the knowledge of the relation between signal attenuation and distance.

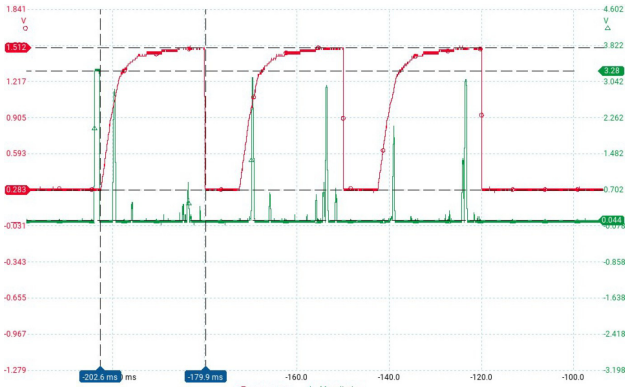

Figure 58. Dynamic Gain, Echo Magnitude

Reverberation

As a part of diagnosis, we observe the control signal of the piezoelectric transducer followed by reverberation (red). Impedance signal (blue) characterizes the sensor's response to stimuli, and it is valuable information for diagnosing internal sensor faults, polluted surface, or detached state.

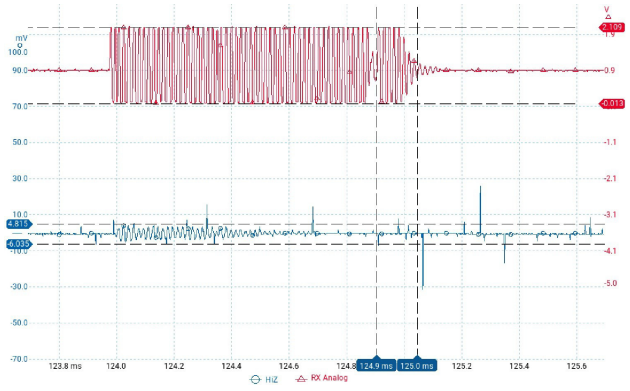

Figure 59. 140 μs Reverberation

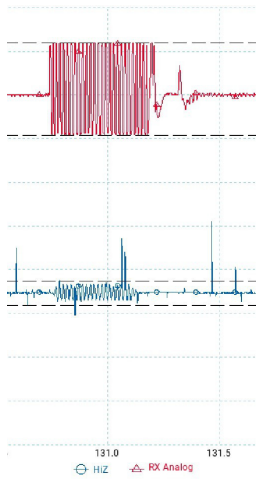

Figure 60. Detached Sensor

Provided evaluation software can be used to measure reverberation without oscilloscope. Register 1 (REG1) in EEPROM memory is a designated area that stores this value. The supported frequency range of the transducer is 30−95 kHz. Below we analyze the reverberation time with different carrier frequencies (TX−RX Period, REG2A) and burst pulse count (TX Pulses, REG3) given the default current of 350 mA. When the nominal resonant frequency of the transducer (orange) is juxtaposed, it almost overlaps with the lowest reverberation time. This indicates that the system is calibrated well to the nominal frequency. The pulse count's impact on the reverberation stays constant from 8 pulses onwards and it changes by 450 ns between 0 and 31 pulses.

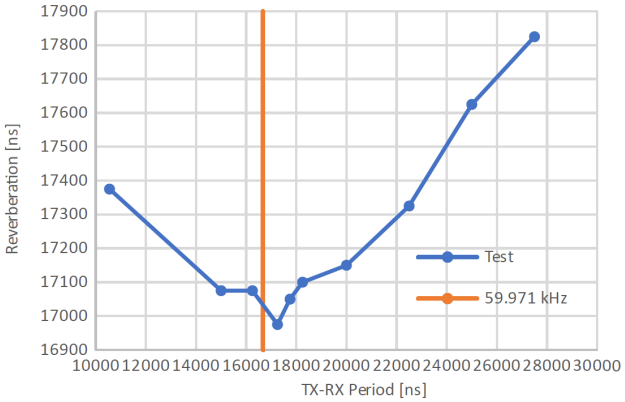

Figure 61. Reverberation vs TX Frequency

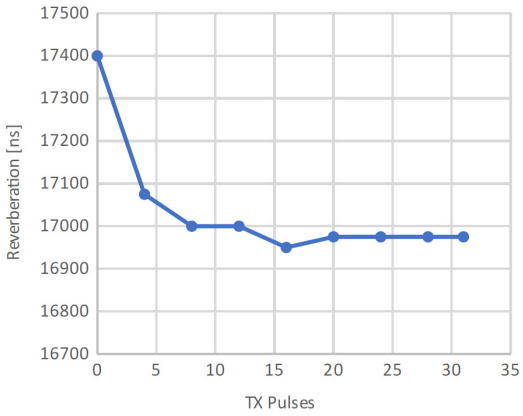

Figure 62. Reverberation vs Burst Pulses

It is recommended to calibrate the system according to the nominal frequency of the transducer. The second calibration step should focus on the measurement range expected in the field. Detection and reaction time at 0.25 m can be improved by lowering the number of pulses and dynamic gain in contrary to 4 m, which requires more transmit energy and higher sensitivity/RX gain of the receiver.

RX Signal Processing & IO Line Communication

The analog signal is processed through several analog and digital stages before an object is. Using provided test pins (TST2, TST3) we can observe selected intermediate signals.

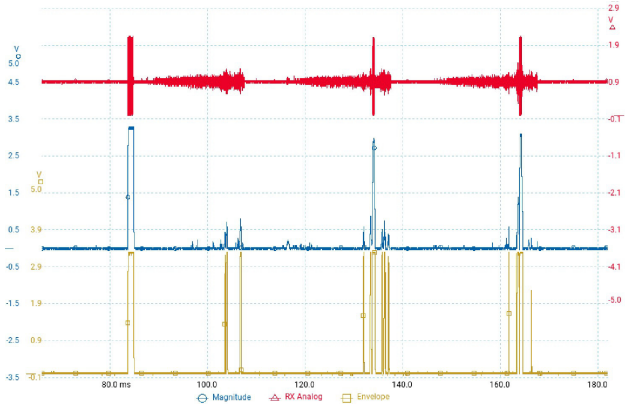

Figure 63. Analog Echo Signal is Amplified and Processed Digitally

Detection signal is a square−shaped pulse of variable duration that is directly encoded onto IO−Line. It resembles a binary signal that indicates either the presence or absence of an object at a certain distance.

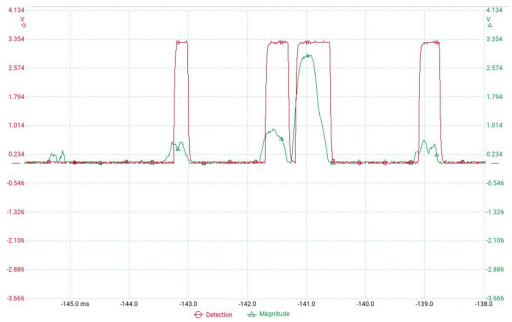

Figure 64. Echoes with Magnitude below Threshold are Discarded

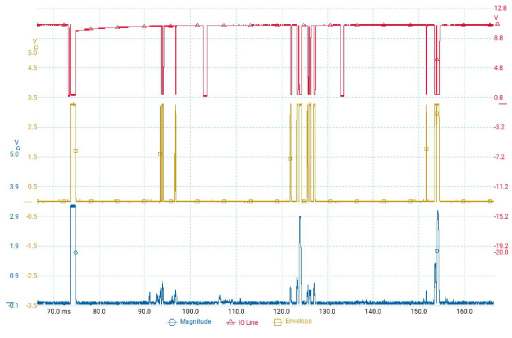

Figure 65. Detected Echoes are Encoded onto IO Line

Measurement with Multiple Sensors

The test setup consists of 3 sensors and 1 object. Every cycle consists of 3 measurements during which 1 sensor acts as a transmitter. To detect an object, i.e., label it with a dot as shown later, any 2 out of 3 sensors should confirm its presence. The role of transmitting sensor rotates between all 3 of them in round−robin fashion (blue, red, yellow spike). The data frames are sent to the central master unit via IO−Line after each measurement cycle.

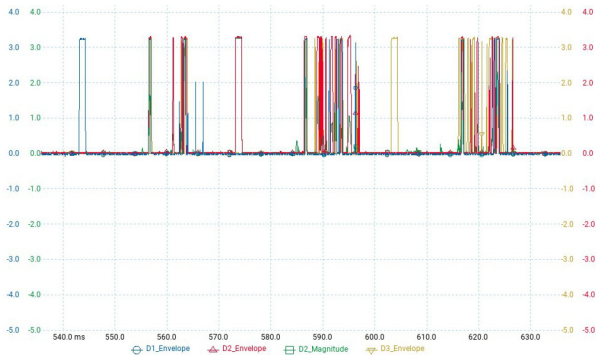

Figure 66. Echo Envelopes for 3 Sensors. S1, S2, S3 Transmit Burst Pulses

During 1 cycle each sensor performs 1 direct (TX & RX) and 2 indirect (RX only) measurements. Two sensors are sufficient to confirm an object.

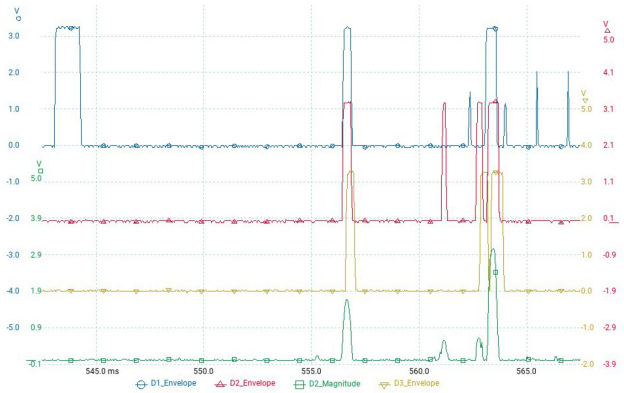

Figure 67. Echo Envelopes for 3 Sensors. S1 Transmits Burst Pulse

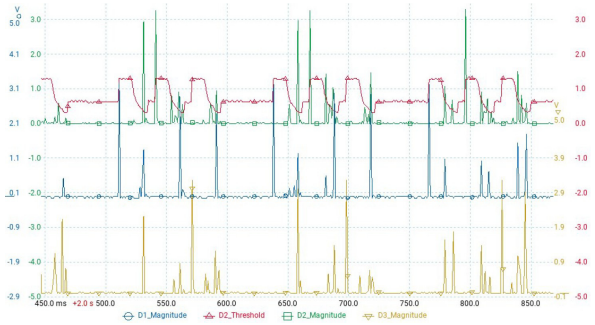

Figure 68. Echo Magnitude Signals compared to the Threshold Value

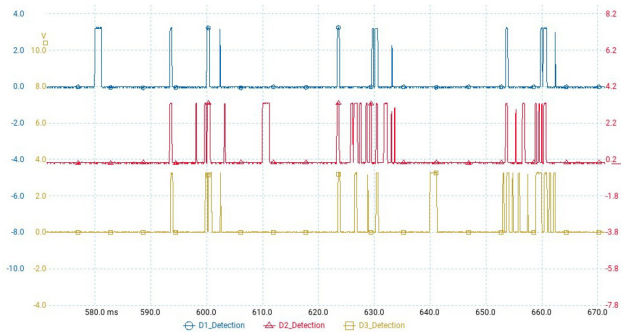

Figure 69. Echo Detection Signals from 3 Sensors

Visualization – Double Confirmation

Objects reported by solely 1 sensor are labelled as unconfirmed and are visualized by a blue arch with the radius of the measured distance.

If an overlapping point of 2 arches is found in 2 consecutive measurements, the point is labelled with a dot. This indicates that trilateration algorithm determined the object's exact position (within the tolerance range) by confirming the distance with 2 sensors.

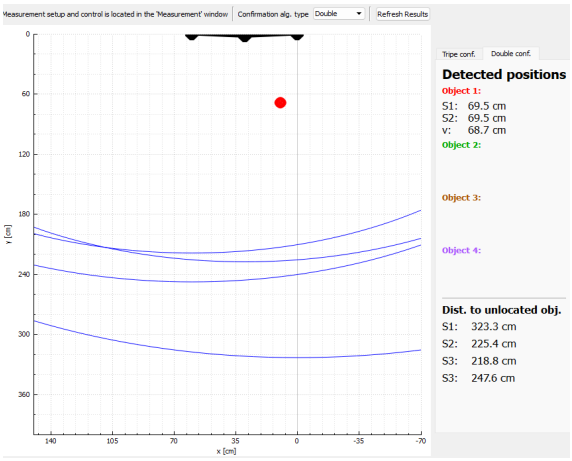

Figure 70. Pole 70 cm away, Visualization, Correct

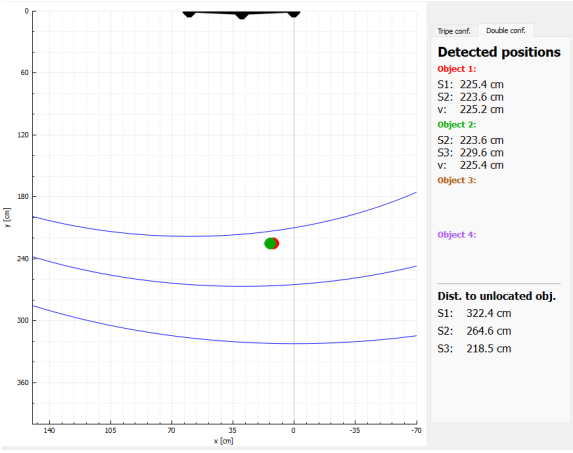

Figure 71. Pole 2.3 m away, Visualization, Duplicate

With more relaxed values of the confirmation tolerances the system's response time might be faster. This comes at the cost of accuracy. Side−effects might occur if an object is moving, or it has a complex/uneven surface. In such a case 2 pairs of sensors might detect the same object at slightly various locations which leads to duplicates. The visualizations were performed for default measurement settings.

Triple Confirmation

The detection with 3 sensors in 2 consequent measurements is more demanding in terms of object's shape. Especially asymmetrical shapes might seem problematic to confirm. Therefore, it is recommended that sensors face the critical area directly and not under an angle. In Figure 72 and Figure 73 we highlight two different behaviors of the algorithm without a change in placement or configuration.

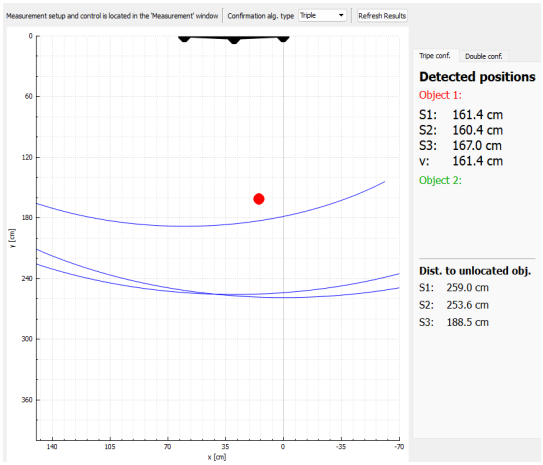

Figure 72. Chair 160 cm away, Detected

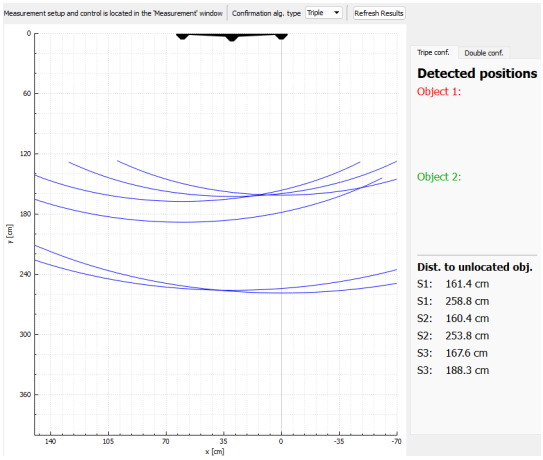

Figure 73. Chair Detection Failed

Measurement data containing echo magnitude is stored in Register 12 (REG12) and is plotted underneath.

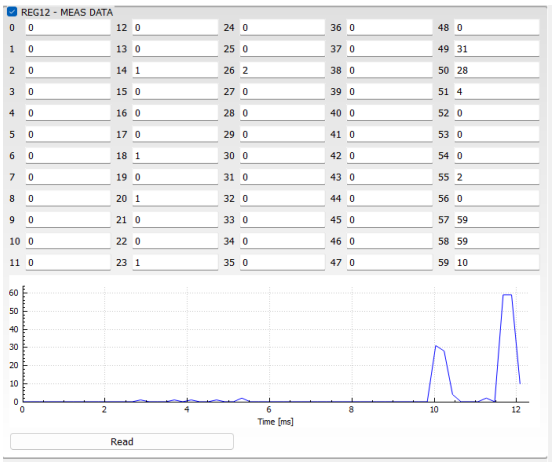

Figure 74. Measurement Data in EEPROM

As discussed previously, double confirmation suffers from side−effects such as duplicates. This can be mitigated with the triple confirmation algorithm if its shortcomings are acceptable in targeted use−case. Below we depict how both algorithms perform in the case of the chair placed centrally at 160 cm.

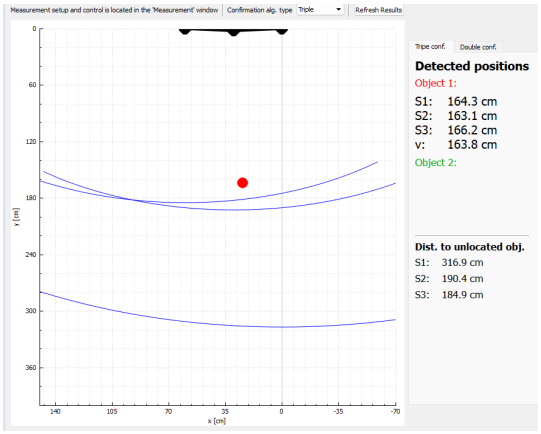

Figure 75. Single Object Detected, Triple Conf. Alg.

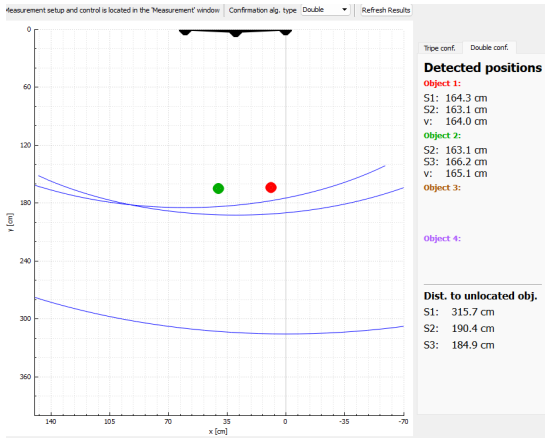

Figure 76. Mirrored Detection from 2 Pairs of Sensors, Double Conf. Alg.

Transformer Characteristics

We analyze input and output voltage signal of the center−tapped transformer. It receives burst pulses with transducer frequency of 56 kHz from TX driver. Voltage is stepped up according to the transformer ratio and current drops accordingly from the set value of 350 mA.

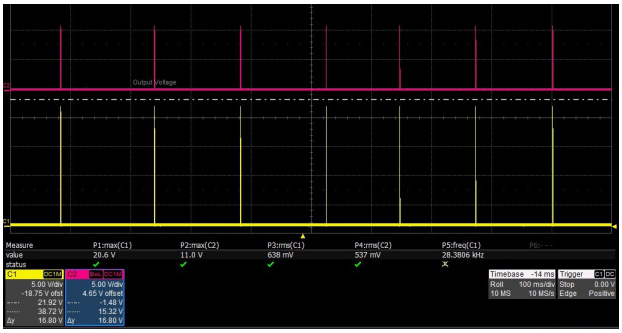

Figure 77. TX Driver Output Pins DRVC (center−tap, C2−purple), DRVA/B (top/bottom, C1−yellow)

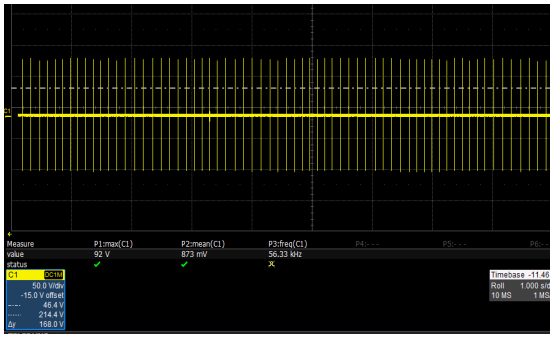

Figure 78. Transducer Input Signal

Expected theoretical transducer voltage can be calculated according to the previously presented formula. The step−up ratio based on the measured voltages is equal to N = 8.36.

LIST OF ABBREVIATIONS

HW	– Hardware
SW	– Software
TX	– Transmitter
RX	– Receiver
TOF	– Time of Flight
SPL	– Sound Pressure Level
ASSP	– Application Specific Standard Product
ASIC	– Application Specific Integrated Circuit
ECU	– Electronic Control Unit
MCU	– Microcontroller Unit
DSP	– Digital Signal Processing
BPF	– Band Pass Filter
LNA	– Low Noise Amplifier
VGA	– Variable Gain Amplifier
EMF	– Electromagnetic Field
EMC	– Electromagnetic Compatibility
SNR	– Signal Noise Ratio
EVK	– Evaluation Kit
EVB	– Evaluation Board
PWM	– Pulse Width Modulation
UART	– Universal Asynchronous Receiver−Transmitter
EEPROM	– Electrically Erasable Programmable Read−Only Memory
PCB	– Printed Circuit Board
BOM	– Bill of Materials
IO	– Input Output
REG	– Register
GND	– Ground
DRV	– Driver

APPENDIX 1

```
//Algorithm utilizing all 3 sensors
    /******** Obstacle confirmation algorithm ********/
    int meas = 1;
    int sensor = 1;
    for(int curr_dir=0; curr_dir<4; curr_dir=curr_dir+2)           //Step1 - get one of the direct distances measured in meas.2 by sensor
    {
        double M2_dir = Distances[meas][sensor][curr_dir];         //Save it as current direct
        qDebug() << "__Triple conf. Algorithm__" << M2_dir;
        qDebug() << "M2_dir" << M2_dir;

        for(int curr_ind_swp1=0; curr_ind_swp1<2; curr_ind_swp1++)  //Step2 - compare indirect meas. measured by sensor 1 in meas.2 with di
        {                                                           //[only indirects calculated by subtracting M2_dir]
            for(int prev_dir=0; prev_dir<4; prev_dir=prev_dir+2)
            {
                if((qAbs(Distances[meas][sensor-1][curr_dir+curr_ind_swp1]-Distances[meas-1][sensor-1][prev_dir]) <= TOLERANCE))
                {
                    qDebug()<< "*first confirmation";
                    qDebug()<< "indirect meas. measured by sensor 1 in meas.2 = direct meas. in meas. 1" << "- Indirect" << curr_dir+curr_i
                    //Step3 - Now compare indirect meas. measured by sensor 3 in meas. 2 with direct meas. in meas. 3
                    for(int curr_ind_swp3=0; curr_ind_swp3<2; curr_ind_swp3++)   //[only indirects calculated by subtracting M2_dir]
                    {
                        for(int next_dir=0; next_dir<4; next_dir=next_dir+2)
                        {
                            if((qAbs(Distances[meas][sensor+1][curr_dir+curr_ind_swp3]-Distances[meas+1][sensor+1][next_dir]) <= TOLERANCE))
                            {
                                qDebug()<< "*second confirmation";
                                qDebug()<< "indirect meas. measured by sensor 3 in meas. 2 = direct meas. in meas. 3" << "- Indirect" << cur
                                //Step4 - compare indirects measured by sensor 2 in meas. 1 with M2_dir
                                for(int prev_ind_swp=0; prev_ind_swp<2; prev_ind_swp++)
                                {
                                    if((qAbs(Distances[meas-1][sensor][prev_dir+prev_ind_swp]-M2_dir) <= TOLERANCE))
                                    {
                                        qDebug()<< "*third confirmation";
                                        qDebug()<< "indirect measured by sensor 2 in meas. 1 = M2_dir" << "- Indirect" << prev_dir+prev_ind_
                                        //Step5 - compare indirects measured by sensor 2 in meas. 3 with M2_dir
                                        for(int next_ind_swp=0; next_ind_swp<2; next_ind_swp++)
                                        {
                                            if((qAbs(Distances[meas+1][sensor][next_dir+next_ind_swp]-M2_dir) <= TOLERANCE))
                                            {...
                                            }
                                        }
                                    }
                                }
                            }
                        }
                    }
                }
            }
        }
    }
```

Obstacle position is now confirmed by several measurements from 3 sensors

Figure 79. Triple Confirmation Algorithm in C++

APPENDIX 2

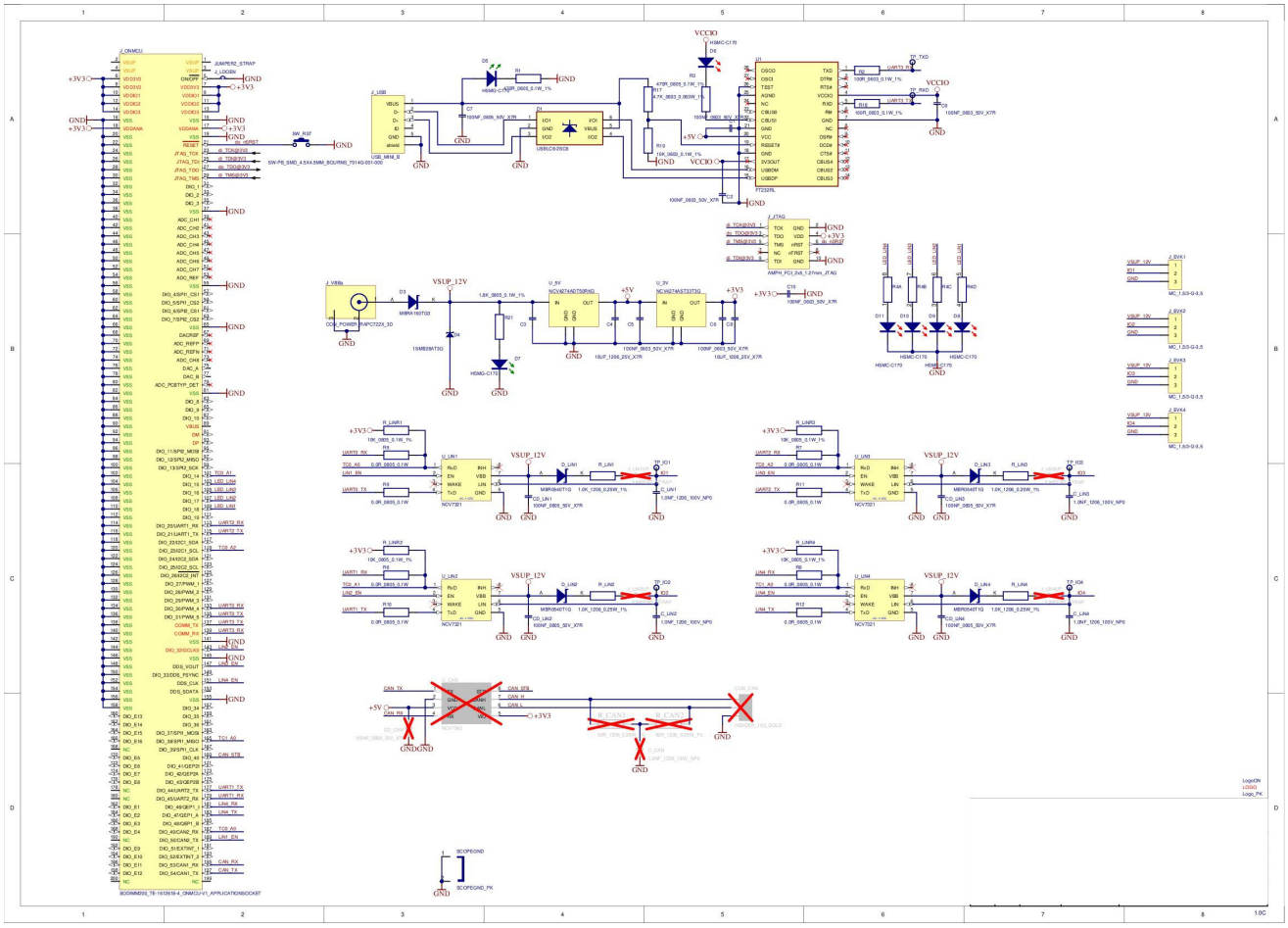

Figure 80. Master Board Schematic

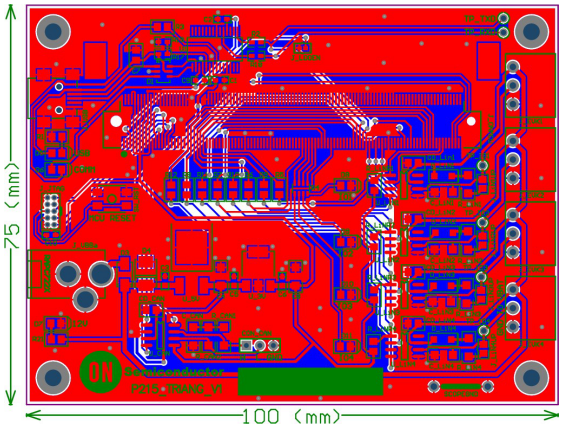

Figure 81. Master Board Dimensions

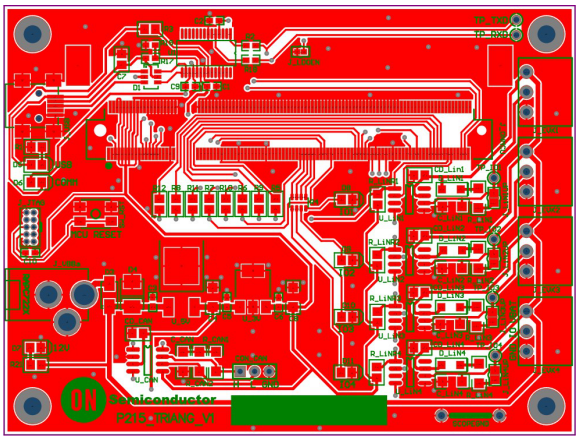

Figure 82. Master Top View

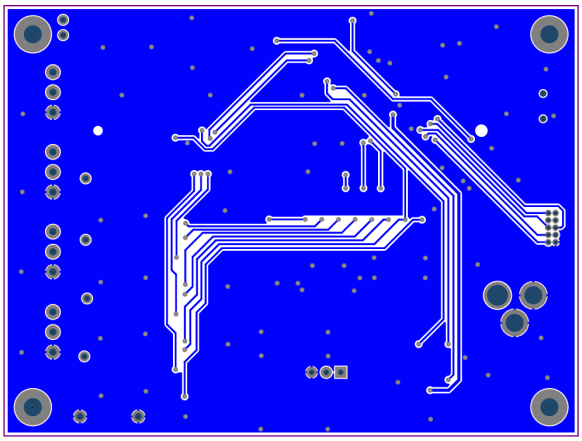

Figure 83. Master Bottom View

APPENDIX 3

Table 4. SENSOR BOARD/SLAVE BILL OF MATERIALS

Description	Quantity
102−3035 SIL SOCKET 2 pins, matches 102−2218 header (made of breakaway SIL32 socket); D01−9973242; HARWIN; RoHS=Yes (repl. for 366−5707, 176−371)	2
109−7981 SCOPEGND; WIRE BRIDGE, made of 1/36 FCI - 75160−105−36LF - HEADER, 1ROW, 36WAY	1
114−0813 RESISTOR NB_0805_1.22K_0.1W_0.1%; RN73C2A1K21BTG ; TYCO; RoHS=Yes	1
116−9632 SMA RIGHT ANGLE JACK GOLD plated; 19−49−5−TGG; MULTICOMP; RoHS=Yes	1
145−9029 DIODE; SWITCHING 200 mA/75V; BAS16HT1G; **onsemi**	1
171−4769 Capacitor 100uF/50V, low ESR=0.18R; EEEFP1H101AP; PANASONIC; RoHS=Yes	1
175−9285 Capacitor MLC−X7R_0805_680pF_10%_100V; MCCA000404; MULTICOMP; RoHS=Yes	2
175−9293 Capacitor MLCC−X7R_0805_4.7NF_10%_100V; MCCA000411; MULTICOMP; RoHS=Yes	1
301−9846 Capacitor MLC−X7R_0805_330pF_10%_50V; 2238 580 15616; PHYCOMP; RoHS=Yes	1
301−9858 Capacitor MLC−X7R_0805_470pF_10%_50V; 2238 580 15618; PHYCOMP; RoHS=Yes	4
301−9949 Capacitor MLC−X7R_0805_100nF_10%_50V; 2238 580 15649; PHYCOMP; RoHS=Yes	3
933−2375 RESISTOR MF_0805_100R_0.1W_1%_100V; MC 0.1W 0805 1% 100R; MULTICOMP; RoHS=Yes (repl. For 911−732)	2
933−2383 RESISTOR MF_0805_1K0_0.1W_1%_100V; MC 0.1W 0805 1% 1K; MULTICOMP; RoHS=Yes (repl. for 911−859)	2
933−2391 RESISTOR MF_0805_10K_0.1W_1%_100V; MC 0.1W 0805 1% 10K; MULTICOMP; RoHS=Yes (repl. For 911−975)	5
933−3150 RESISTOR MF_0805_390R_0.1W_1%_100V; MC 0.1W 0805 1% 390R; MULTICOMP; RoHS=Yes (repl. For 911−800)	1
CUSTOM TRAFO SMD, primary 3 leads, secondary 2 leads	1
DK:277−2415−ND CONNECTOR HEADER, PCB, HORIZONTAL, 3.5MM, 300V/8A, 3WAY; MC 1,5/3−G−3,5 (1844223); PHOENIX CONTACT; RoHS=Yes	1
DK:277−5789−ND CONNECTOR HEADER, PCB, HORIZONTAL, 3.5MM, 300V/8A, 5WAY; MC 1,5/5−G−3,5 (1844249); PHOENIX CONTACT; RoHS=Yes	1
DK:277−2413−ND PLUG SCREW, 3.5MM, 3WAY; MC 1,5/3−ST−3,5; PHOENIX CONTACT; RoHS=Yes	1
DK:277−5721−ND PLUG SCREW, 3.5MM, 5WAY; MC 1,5/5−ST−3,5; PHOENIX CONTACT; RoHS=Yes	1
onsemi P215 ultrasonic ASSP, IO; TSSOP16; NCV75215; **onsemi**	1

APPENDIX 4

Table 5. MASTER BILL OF MATERIALS

Description	Quantity
109−7981 SCOPEGND; WIRE BRIDGE, made of 1/36 FCI - 75160−105−36LF - HEADER, 1ROW, 36WAY	1
109−9786 RESISTOR MF_0805_0R_0.1W_100V; WCR0805−R005JI; WELVYN; RoHS=Yes (repl. for 772−239)	8
110−0192 RESISTOR MF_1206_1K0_0.25W_1%_200V; WCR 1206 1K 1%; WELWYN; RoHS=Yes (repl. for 420−384)	4
114−6032 USB TO UART; FT232RL; FTDI; RoHS=Yes	1
126−9406 Very low capacitance ESD protection; USBLC6−2SC6; ST Microelectronics; RoHS=Yes	1
128−8255 Capacitor MLC−X7R_0603_100NF_10%_50V; C0603C104K5RAC; KEMET; RoHS=Yes	7
143−1076 DIODE SCHOTTKY 60V/1A; MBRA160TG3; SMA; **onsemi**; RoHS=Yes	1
146−9752 RESISTOR MF_0603_100R_0.1W_1%_75V; CRCW0603100RFKEA; VISHAY; RoHS=Yes	2
160−7971 SWITCH SPNO 4.5x4.5 mm; 7914G−001−000; BOURNS; RoHs=Yes	1
160−8727 SOCKET, PCB, DC POWER, 2.1MM, 5A, 250V; RAPC722X; SWITCHCRAFT; RoHS=Yes	1
186−5285 HEADER, 1.27MM, Through−hole, 10WAY, 20021111−00010T4LF, AMPHENOL FCI	1
192−4881 LDO, 400MA, 3.3V, NCV4274AST33T3G, SOT223, **onsemi**	1
192−4884 LDO, 400MA, 5V, NCV4274AST50T3G, TO−252, **onsemi**	1
209−4044 C_MLC−X7R_1206_10UF_10%_25V; 12063C106KAT2A; AVX; RoHS=Yes	2
239−6418 TE−1612618−4; AMP 1612618−4 CONNECTOR, DIMM SOCKET, 200POS; SODIMM200; TE	1
301−9949 Capacitor MLC−X7R_0805_100nF_10%_50V; 2238 580 15649; PHYCOMP; RoHS=Yes	5
499−316 Capacitor MLC−NP0_1206_1nF_5%_100V; 12061A102JAT2A; AVX; RoHS=Yes (repl. for 355−4983)	4
579−0852 LED DIODE GREEN 20mA, 0805; HSMG−C170; AVAGO TECHNOLOGIES; RoHS=Yes	2
855−4501 LED DIODE RED 20mA, 0805; HSMC−C170; AVAGO TECHNOLOGIES; RoHS=Yes	5
873−1128 (PK100) TESTPIN 200 SER. HOLE 1.0 BLACK; 20−2137; VERO; RoHS=Yes (repl. for 240−333)	6
923−4489 RESISTOR ARRAY 330R_1206_0.063W_5%; 235003510331; PHYCOMP; RoHS=Yes	1
923−8603 RESISTOR MF_0603_10KR_0.1W_1%_50V; RC0603FR−0710KL; PHYCOMP; RoHS=Yes	1
933−1247 RESISTOR MF_0603_4.7KR_0.063W_1%_50V; MC 0.063W 0603 1% 4k7; MULTICOMP; RoHS=Yes	1
933−2391 RESISTOR MF_0805_10K_0.1W_1%_100V; MC 0.1W 0805 1% 10K; MULTICOMP; RoHS=Yes (repl. for 911−975)	4
933−2715 RESISTOR MF_0805_1K8_0.1W_1%_100V; MC 0.1W 0805 1% 1K8; MULTICOMP; RoHS=Yes (repl. for 911−884)	1
933−3258 RESISTOR MF_0805_470R_0.1W_1%_100V; MC 0.1W 0805 1% 470R; MULTICOMP; RoHS=Yes (repl. for 911−811)	2
955−6923 DIODE SCHOTTKY 40V/0.5A; MBR0540T1G; **onsemi**; RoHS=Yes	4
1753806 MINI USB B, RECEPTACLE, SMT, MUSB−05−S−B−SM−A, SAMTEC	1
DK:277−2415−ND CONNECTOR HEADER, PCB, HORIZONTAL, 3.5MM, 300V/8A, 3WAY; MC 1,5/3−G−3,5 (1844223); PHOENIX CONTACT; RoHS=Yes	4
onsemi DIODE TVS 600W, bidirectional, Vb=28V; 1SMB28AT3G; **onsemi**; RoHS=Yes	1
onsemi NCV7321; Stand−alone LIN Transceiver, −40.+125C, SOIC8; **onsemi**	4

ADDITIONAL INFORMATION

TECHNICAL PUBLICATIONS:
Technical Library: www.onsemi.com/design/resources/technical−documentation
onsemi Website: www.onsemi.com

ONLINE SUPPORT: www.onsemi.com/support
For additional information, please contact your local Sales Representative at www.onsemi.com/support/sales